

Data acquisition system of a flexible solar collector

Ramy Hattab

Dissertation submitted to Escola Superior de Tecnologia e Gestão de Bragança to obtain the Degree of Master in Industrial Engineering, Mech. Engineering branch under the scope of the double diploma with Université Libre de Tunis

Supervised by

Professor Luís Manuel Ribeiro
Professor Emna Rebhi ben Fguir

This dissertation does not include the comments and suggestions mentioned by the Jury

Bragança

2020

Acknowledgements

I would first like to thank my thesis advisor professor Luís Manuel Frölen Ribeiro of the Escola Superior de Tecnologia e Gestão at Instituto Politécnico de Bragança. The door to Prof. Frölen office was always open whenever I ran into a trouble spot or had a question about my research or writing. He consistently allowed this paper to be my own work, but steered me in the right the direction whenever he thought I needed it.

I would also like to acknowledge professor Emna Rabhi ben Feguir of the Institut Supérieur Polytechnique Privé at Université Libre de Tunis as the second reader of this thesis, and I am gratefully indebted to her for her very valuable comments on this thesis.

Finally, I must express my very profound gratitude to my parents for providing me with unfailing support and continuous encouragement throughout my years of study and through the process of researching and writing this thesis. This accomplishment would not have been possible without them. Thank you.

Abstract

The aim of this Master Thesis work is to create a weather station based on sensors by creating a data acquisition system with LabView in purpose to collect data for solar collector based on the European standard for solar collector testing. EN 12975-2(CEN 2006) offers two different methods for characterizing the thermal performance of solar thermal collectors: The steady state (SS) method and the quasi-dynamic method (QDT).

The process of building the data acquisition system begin by choosing thermocouples and NI USB-6008 DAQ device to measure ambient temperature, LM35 sensor and NI myDAQ for the inlet mass flow measurement, for the surrounding air speed we used vernier anemometer with NI myDAQ, another thermocouple type k for surrounding air temperature measurement and a pyranometer with NI USB-6008 for global and diffuse irradiance.

Hence,

The main action of data acquisition systems is the sampling signals that measure real world physical conditions (voltage, current) and converting the resulting samples into digital values that can be handled, for example, by a computer. This project describes the fundamental concepts of data acquisition systems; in particular sensors, transducers, communication cabling, and system configurations.

1	Introduction	1
2	Theoretical framework	2
2.1	Solar theory	2
2.2	Solar radiation	2
2.3	Sun position relative to the collector surface	3
3	Materials and methods	6
3.1	Main parts of solar water heater	6
3.2	Measurements of the collector performance	9
3.3	Steady-state test	10
3.3.1	Dependence of tilt angle	11
3.3.2	Solar radiation simulator for steady-state efficiency test	12
3.4	Quasi-dynamic test	13
3.5	Test period and procedure	16
3.6	Installation required for measurements	18
3.6.1	Data acquisition	18
3.6.2	Thermocouples	21
3.6.3	Ambient temperature	31
3.6.4	Inlet mass flow	33
3.6.5	Surrounding air speed	34
3.6.6	Surrounding air temperature	28
3.6.7	Azimuth and tilt angle	30
3.6.8	Incident angle of direct radiation	31
3.6.9	Global, direct and diffuse irradiance	34
3.6.10	Incident longwave radiation	36

3.7	Weather station	37
3.7.1	Capricorn 2000EX weather station	37
3.7.2	The weather MicroServer	37
3.8	Data collection from the weather station	37
3.8.1	Developing the application to save weather station data	38
4	Discussion.....	40
4.1	sensors	40
4.2	DAQ hardware.....	40
4.3	Signal conditioning.....	41
4.3.1	Sensor cables:	41
4.3.2	Digital isolation:	41
4.3.3	Analogue isolation:	42
4.3.4	Low-pass filtering:	42
4.3.5	Amplifiers:	42
5	Conclusions and future work.....	43
6	References	44

List of tables

Table 1: Guiding for the spectral distribution in a solar simulator 13

Table 2: Highest fluid outlet temperature as a function of collector type..... 15

Table 3: Test condition 15

Table 4: Mean fluid temperature and weather condition per day type 15

Table 5: Required variable measurements..... 15

Table 6: Test condition and permitted deviations..... 17

List of figures

Figure 1: The different solar and collector angles.....	5
Figure 2: The incidence angle and the different collector angles.....	5
Figure 3: Evolution of the developed collectors.....	7
Figure 4: Layer of channels (model4).....	7
Figure 5: Perspective view of the model.....	8
Figure 6: Temperature measurement points.....	9
Figure 7: The appearance of NI myDAQ.....	20
Figure 8: The appearance of NI myDAQ.....	21
Figure 9: Thermocouple junction diagram.....	22
Figure 10: SCXI-1303 parts locator diagram.....	24
Figure 11: Thermocouple connected to channel 0 of the SCXI-1303 Terminal Block.....	24
Figure 12: Connecting the SCXI-1303 Terminal Block to the SCXI-1102 Module.....	25
Figure 13: Complete installation.....	25
Figure 14: VirtualBench-Logger Main Run-Time Window.....	28
Figure 15: VirtualBench-Logger Setting Window.....	29
Figure 16: Block diagram of thermocouple type k.....	30
Figure 17: Front panel thermocouple type k.....	30
Figure 18: Block diagram of ambient temperature.....	32
Figure 19: Front panel of ambient temperature.....	32
Figure 20: Block diagram of flow meter SLA5800.....	33
Figure 21: Front panel of flow meter SLA5800.....	34
Figure 23: Front panel of surrounding air speed.....	35
Figure 22: Block Diagram of surrounding air speed.....	27
Figure 24: Block diagram of surrounding air temperature.....	29

Figure 25: Front panel of surrounding air temperature	29
Figure 26: Block diagram of the pyranometer	35
Figure 27: Front panel of the pyranometer.....	35
Figure 28: Bloc diagram for the weather station data	38

1 Introduction

The working principle of solar collectors is to absorb solar radiation, convert it into thermal energy, and then transmit it so that it can be used for heating. hence, we will collect data by creating a weather station based on manipulating transducers through data acquisition system based on the EN 12975 standard.

the EN 12975 allows for tow alternative test methods. the steady-state test method and the quasi-dynamic test method.

Basically, the two methods have the same requirements for suitable test data. Therefore, the recommended test sequence will be obtained and cut out those measurement data sequences corresponding to the steady-state requirements, and regular steady-state parameters can also be performed. Recognition. However, the test database must of course contain more information and appropriate information in order to be able to identify.

Data acquisition systems are widely used in renewable energy sources to collect data on the performance of installed systems for evaluation. The proposed system consists of a set of sensors for measuring metrological parameters.

The collected data are first conditioned using precision electronic circuits and then interfaced to a PC using a data-acquisition card. The LABVIEW program is used to further process, display and store the collected data in the PC disk. The proposed architecture permits the rapid system development and has the advantage of flexibility in the case of changes, while it can be easily extended for controlling the system operation.

First, we will identify the components of the solar water heater system, then choose the transducers needed to collect measurement from the solar collector. The LABVIEW programs will be the interface between user and sensors to manipulate the system and change parameters when need to.

Finally, we explain the steady-state and quasi-dynamic tests process and how to explore the sensors used above to collect data required to evaluate solar collector performance based on the EN 12 975 standard.

2 Theoretical framework

The following section describes the analytical and experimental method used when evaluating thermal performance of solar collectors.

The main goal for test methods of solar collectors is to characterize the behavior of a collector as accurately as possible regarding its energy thermal performance and durability. Solar collector depends on many factors such as the weather conditions, the materials or the fluid properties, there is a requirement for finding valid coefficients that can illustrate the collector performance for a wide range of conditions and collector's types.

The proposed software tool integrates several types of instruments into a system which is able to offer dynamic measurements to collect data using precision electronic circuits and then interfaced to a personal computer using data-acquisition modules. The National Instrument (NI) LabVIEW program is used to process, display and store the collected data.

2.1 Solar theory

For explaining the principles behind the absorption of the solar radiation by solar collectors, some basic properties regarding the sun position are needed. Most of the theory is explained in detail in solar Engineering of Thermal Processes, Second Edition (Duffie & Beckman, 1991). However, it is interesting here to sum up some of the important points mentioned in this book for a better understanding of the calculations later on.

2.2 Solar radiation

When considering a surface receiving sun radiation, three types of radiation can be distinguished. Firstly, the beam (also called direct) radiation G_b is the radiation received from the sun without having been scattered by the atmosphere. Secondly, the diffuse radiation G_d is the one received after the sun radiation direction has been changed when scattering in the atmosphere. Finally, the total radiation is the sum of beam and diffuse radiation received on the collector surface. The fraction of beam and diffuse radiation received will mainly depend on the weather conditions and the sun position in the sky.

2.3 Sun position relative to the collector surface

To evaluate the direction of the incident beam radiation on the surface, a couple of parameters need to be introduced for determining the sun position relative to the collector surface.

Firstly, the position of the surface on earth must be known. It will be identified via the longitude L or the angular location from the prime meridian and the latitude ϕ , i.e. the angular location of the equator with north positive. Then, the solar time can be distinguished from the standard time. It is defined as the time based on the apparent angular motion of the sun across the sky, with solar noon being the time when the sun crosses the meridian of the observer.

Used in all the sun-angle relation, it can be expressed according to Equation (1)

$$\text{Solar time} = \text{Standard time} + 4 * (L_{st} - L_{loc}) + E \quad \text{Equation 1}$$

Here, L_{st} is the standard meridian for the local time zone in degrees west and L_{loc} is the longitude of the observer in degrees west. E is in minutes and given by Equation (2),

$$E = 229.2 * (0.000075 + 0.001868 * \cos(B) - 0.032077 * \sin(B) - 0.014615 * \cos(2B) - 0.04089 * \sin(2B)) \quad \text{Equation 2}$$

When B is given by Equation (3) with n the number of the day of the year ($1 \leq n \leq 365$),

$$B = \frac{(n-1)360}{365} \quad \text{Equation 3}$$

Secondly, azimuth are necessary to determine the orientation of the surface; a) the slope β or the angle between the plane of a surface (here the collector) and the horizontal and b) the surface azimuth angle γ , i.e. the deviation of the projection on a horizontal plane of the normal to the surface from the local meridian with zero due south and west positive .

Finally, angles are identified in order to position the sun and determine the beam radiation direction. The hour angle ω will be the angular displacement of the sun due to the earth rotation on its axis 15° per hour. Hence, it is expressed by the Equation, giving a negative angle for the morning and a positive one for the afternoon,

$$\omega = 15 * (\text{solar time} - 12) \quad \text{Equation 4}$$

The angular position of the sun at solar noon must also be known. It is called the declination δ and can be expressed by Equation (5) with respect to the plane of the equator and north positive,

$$\delta = 23.45 * \sin \left(360 * \frac{284+n}{365} \right) \quad \text{Equation 5}$$

The solar altitude angle α_s or the angle between the horizontal and the line to the sun is shown in Equation (6),

$$\alpha_s = \arcsin (\cos(\omega) * \cos(\varphi) + \sin(\delta) * \sin(\varphi)) \quad \text{Equation 6}$$

The angle is the complement of the zenith angle θ_z , i.e. the angle between the vertical and the line to the sun. The relation between those angles is therefore given in Equation (),

$$\theta_z = 90 - \alpha_s \quad \text{Equation 7}$$

A last angle for locating the sun is necessary for further calculation, the solar azimuth angle γ_s , or the angular displacement from south of the beam radiation projection on the horizontal plane. It can be expressed as seen in Equation (), with displacements east of south negative and west of south positive,

$$\gamma_s = \text{SIGN}(\omega) * \left| \arccos \left(\frac{\cos(\theta_z) * \sin(\varphi) - \sin(\delta)}{\sin(\theta_z) * \cos(\delta)} \right) \right| \quad \text{Equation 8}$$

With $\text{SIGN}(\omega) = \begin{cases} 1 & \text{if } \omega \geq 0 \\ -1 & \text{otherwise} \end{cases}$

Most of the previous angles are illustrated in Figure 1.

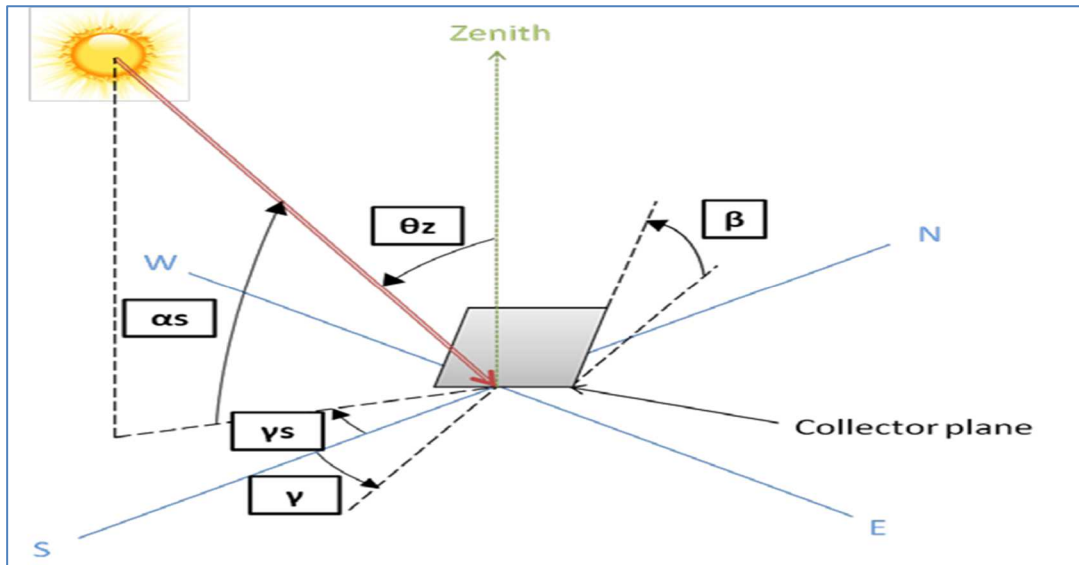


Figure 1: The different solar and collector angles

Now that all the necessary parameters have been identified, a crucial angle using previous data can be introduced; the angle of incidence θ_i or the angle between the beam radiation on a surface (here the collector) and the normal to that surface. This angle will be used later in the calculations especially due to its impact on the radiation received by the collector and can be derived from:

$$\theta_i = \arccos (\cos \theta_z) * \cos(\beta) + \sin(\theta_z) * \sin(\beta) * \cos(\gamma_s - \gamma) \quad \text{Equation 9}$$

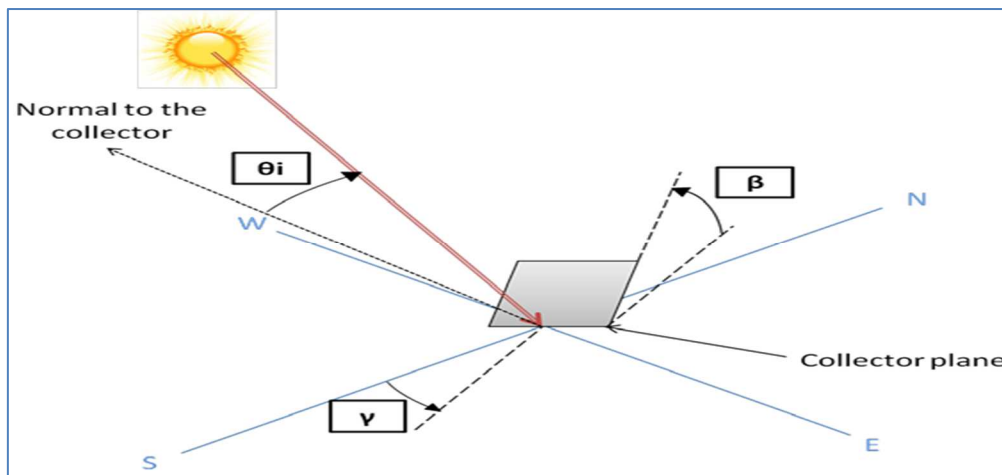


Figure 2: The incidence angle and the different collector angles

(Thornsberry, 1989) (Duffie e Beckman, 1991)

3 Materials and methods

The following section describes the analytical and experimental method used when evaluating thermal performance of solar collectors. It also describes the optimization possibilities found for improving the QDT method.

The solar collector has three parts: the first consists of a transparent cover, which has the function of promoting the greenhouse effect and increasing the temperature on the absorbent surface, the second is collecting plate itself which is responsible for heating the fluid and the third part is the insulating layer whose function is to reduce the thermal losses of the system.

3.1 Main parts of solar water heater

Solar water heater systems are made up of solar collector, storage tanks and piping systems.

- Solar collector: solar collector receives and transfers the solar radiation energy into thermal energy in the working fluid (water).
- System of working fluid channel or pipe: This is the connection between collector and storage tank.
- Hot water tank: This is used to store and maintain hot water. The hottest water on the top and water temperature increase from the bottom to the top of the tank due to thermosiphon effect.

For the collector to be flexible and low cost, the material adopted was polyurethane (PU) film, due to its price, maneuverability and protection against ultraviolet rays (UV). For the numerical simulations, the collector was simulated in a heating system with 15 mm external diameter pipes and a reservoir with a capacity of 150 liters.

In total, four models of solar collectors were designed and non-functional prototype was made. The non-functional prototype was manufactured based on model 2 to analyze the manufacturing processes and problems which were then considered to design model 3.

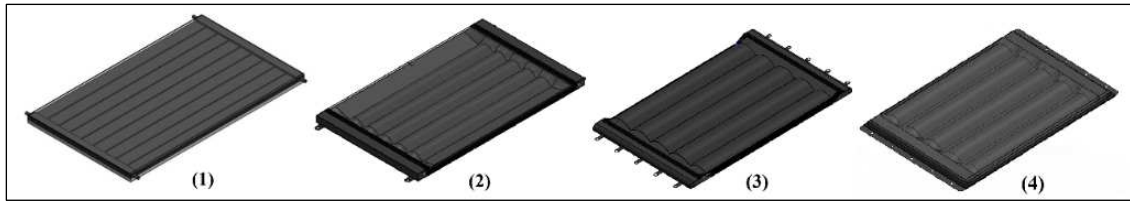


Figure 3: Evolution of the developed collectors

All collector models have an approximate useful area of 0.7 m^2 , with the first model having nine heating channels, the second model having seven, and the third having five. The reduction of channels was made to facilitate construction.

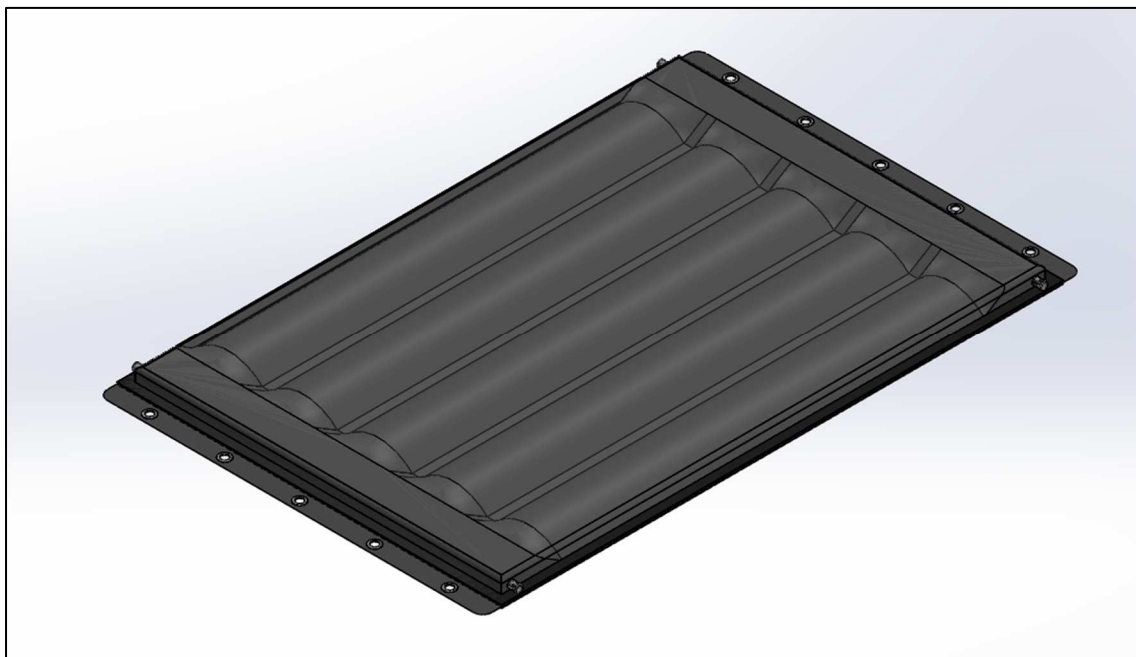
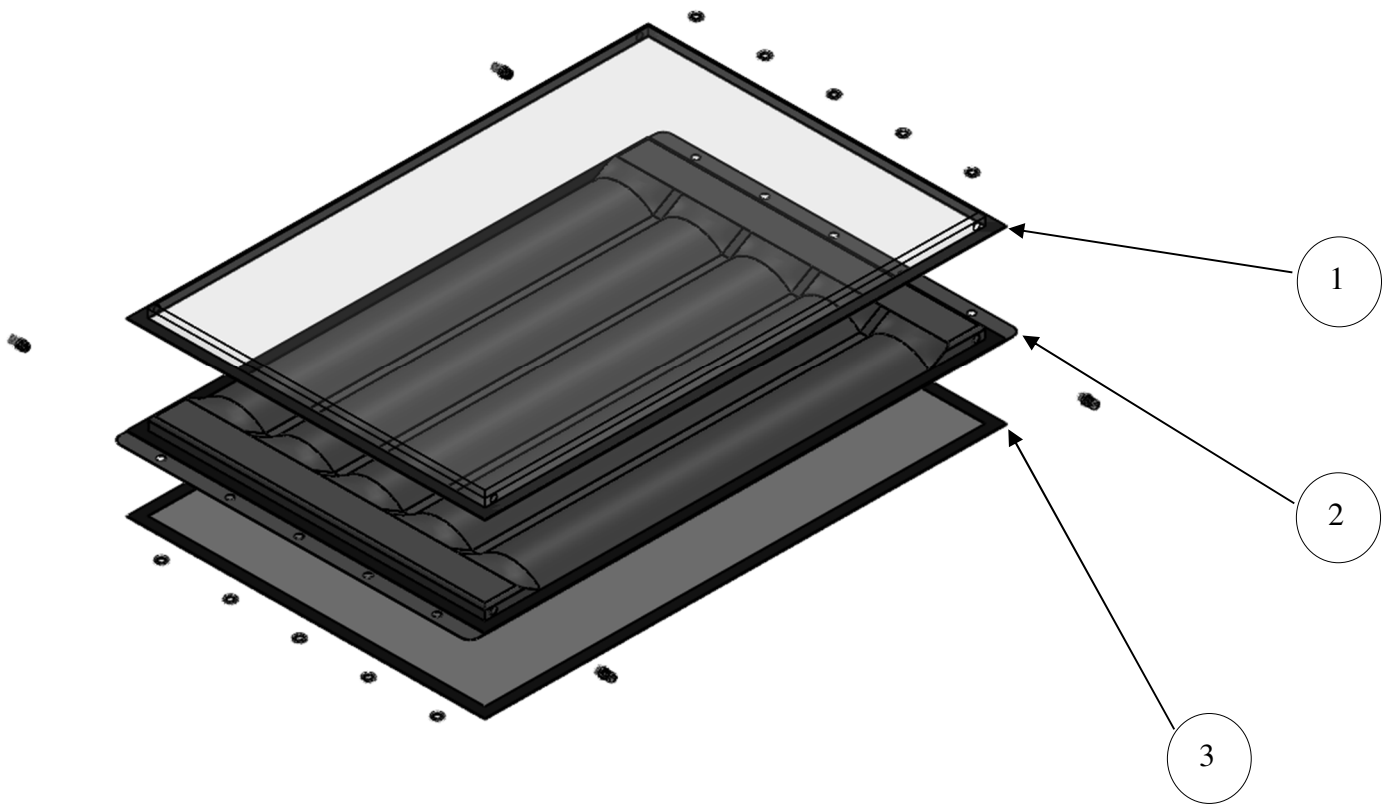


Figure 4: Layer of channels (model4)



1. layer of channels
2. Transparent coverage
3. Insulation cover

Figure 5: Perspective view of the model

The collector is made of black polyurethane fabric, this material was chosen taking into account its affordable price and its UV protection layer, which will provide a longer useful life(Cleber Pizzatto Dallegrave, 2019).

To collect the temperature simulation data in the reservoir, at the outlet and inlet of the collector, five points were instead in the model. Therefore, three collection points were applied to the reservoir, where point P1 is located in central region approximately 5 centimeters below the surface, this point indicates the position in which the tube for collecting heated water for use is installed; the points P2 and P3 are located in the middle and in the lower region of the reservoir in order to calculate the average temperature inside. Point P4 is located at the entrance of the collector (inlet temperature) and point P5 at the outlet (outlet temperature and mass flow).

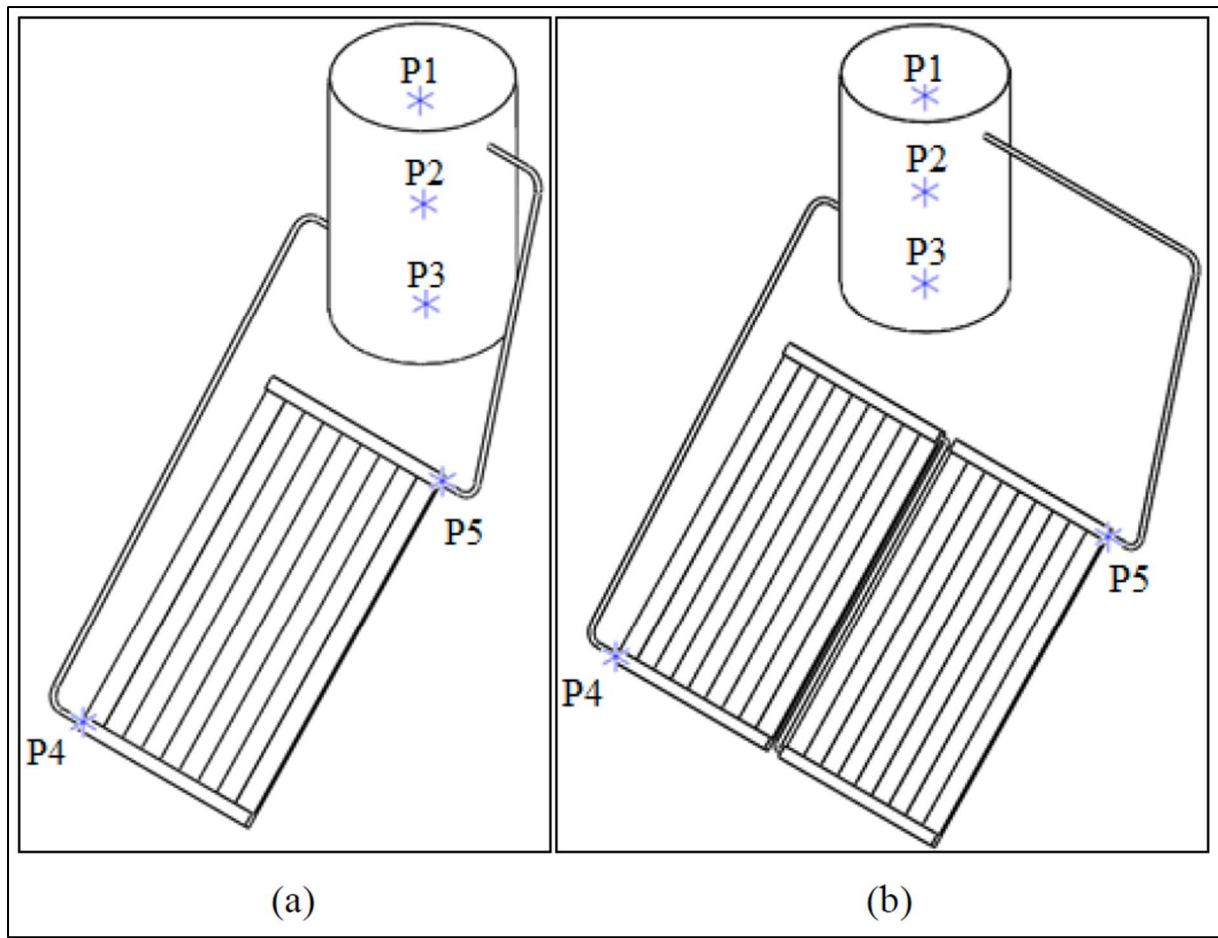


Figure 6: Temperature measurement points

3.2 Measurements of the collector performance

The performance of a solar collector is characterized by the useful gain in power the media acquires while passing through the collector. This can also be illustrated in Eq by the range of temperature between the fluid inlet and outlet

$$Q_{coll} = \dot{m} * C(T_{out} - T_{in}) \quad \text{Equation 10}$$

This equation is the basics for measuring collector performance by exposing the device to solar radiation and at the same time measuring the fluid inlet and outlet temperature as well as the fluid flow rate.

The EN 12975 standard provides two generally different methods to determine the thermal performance of solar collectors: steady-state and quasi dynamic approach, usually referred to as SS and QDT.

To give accurate results on collector performance (actually in terms of heat loss coefficient), the collector should be tested at the highest normal operating temperature as far as possible. For standard applications, this is usually not a problem, and inlet temperatures of 80-90°C can be handled easily. However, for medium and high temperature applications, this can be a problem. If the collector is mainly used for such applications, it should be tested in the laboratory using relevant resources (i.e. a high temperature test rig).

Every collector submitted to a performance test shall be exposed for 5 hours at minimum 700 w/m^2 before the performance test.

3.3 Steady-state test

The three most widely used standards for steady-state testing of glazed solar thermal collectors are ASHRAE 93, ISO 9806-1 and EN 12975-2. All three standards require a collector time constant test, an instantaneous thermal efficiency test, and an incident angle modifier test.

The steady-state method is well-defined, and a lot of experience has been gained from long-term use of this method. Therefore, compared with the QDT method, it has a better understanding of users (i.e. manufacturers and consumers). On sunny days, the steady-state method is also easier to apply. On the other hand, the steady-state method does not consider the influence of air speed and diffuse irradiance, and the test conditions can be considered restrictive with regard to the requirements for clear sky, scattered radiation limitation, normal occurrence of solar radiation and stability of test conditions.

We start to describe the steady-state collector model in the EN 12975 standard. The basic equation for the steady-state model for near normal incidence angle operation can be written as

$$Q = F'(\tau\alpha)_{en}G - c_1(t_m - t_a) - c_2(t_m - t_a)^2 \quad \text{Equation 11}$$

There are furthermore optional, separate test procedures for the determination of incident angle dependence of the zero-loss efficiency, here denoted $k_\theta(\theta)$ and the effective thermal capacitance of the collector, c_5 or $(mC)_e$. The parameter $(mC)_e$ is not measured, but calculated by weighting the capacities of collector components. The full instantaneous equation based on all options can be written as

$$Q = F'(\tau\alpha)_{en}k_{\theta}(\theta) G - c_1(t_m - t_a) - c_2(t_m - t_a)^2 - c_5 \frac{dt_m}{d\tau} \quad \text{Equation 12}$$

This still a clear weather or indoor solar simulator model.

Only high irradiance levels and thus only low diffuse fraction are accepted in the test sequence. It is required that the incident angle is near normal, so that incidence angle effect can be neglected.

This regulation limits the time available for outdoor testing very suitable for outdoor activities in many climates very tested according to the steady-state test method expensive.

The steady-state model has no correction term for diffuse radiation. This is needed in most simulation programmers for long term performance calculations.

The solar radiation must be divided into beam and diffuse radiation and a separate incidence angle correction has to be known for the diffuse radiation.

No correction method for non-stationary testing the conditions are described during the test. Therefore, every test requires stable weather conditions point.

3.3.1 Dependence of tilt angle

- For “abnormal” type collectors, you can first determine the IAM to ensure that the 2% requirement is met.
- During the test, the inclination angle cannot be fixed due to the IAM value required. The tilt angle range during the measurement provides useful and practical information, which can be reported in the test report.
- Heat pipe-based collectors may have a strong tilt dependency, so this must be taken into consideration when testing such collectors. Generally, slopes below 20-30 degrees should be avoided, but this is not a general rule. Free measurement can easily indicate tilt dependence.
- The heat loss coefficient of flat plate collector is also related to the tilt. Therefore, unless the inclination is to be determined, measurements at high temperature (used to determine heat loss) can only be performed at the nominal inclination (2% IAM requirement).

3.3.2 Solar radiation simulator for steady-state efficiency test

The indoor thermal efficiency test under steady state requires the use of a solar simulator. The main technical characteristics to be satisfied are:

A lamp: should be able to produce an average irradiance of at least 700 w/m^2 on the aperture of the collector. Values in the range of 300 w/m^2 to 1000 w/m^2 can also be used for special tests, provided that the accuracy requirements given in the table below.

It is recommended to use a lamp with radiation level of up to 1100 w/m^2 , so that the simulator can also be used for other standard tests, such as high temperature tests. It is important to consider the distance between the collector and the solar simulator to ensure the required radiation level and distribution. It is also hoped that the intensity setting of the light can be controlled separately from the computer. In this way, the radiation pattern on the collector can be seen continuously, and the uniformity of the lamp can be adjusted in a visual and easy way.

Before each efficiency test, the uniformity of the solar simulator must be checked. Usually an automatic X-Y system is used to measure the radiation pattern, which moves the reference pyranometer every 150 mm in both directions. The radiometer is held at each position for approximately 20-30 seconds, and an irradiance map of the area covered by the solar collector is obtained. The difference between the irradiance value of each location and the average irradiation pattern should be less than 15%. It is important to age the bulb at the beginning of its life to stabilize the different components of the bulb. It is also recommended to stabilize the simulator's lights before performing any tests, the time required depends on the type of lights used.

The spectral distribution of the lamp must be measured by a spectrometer, or the characteristics of the lamp must be outsourced to an accredited laboratory. It is difficult to find equipment or laboratories that can measure the spectrum in the range of $0.3 \mu\text{m}$ to $3 \mu\text{m}$, especially $2.5 \mu\text{m}$. It is recommended to take these measurements every time the bulb is replaced. Although the standard does not specify acceptance criteria.

Table 1: Guiding for the spectral distribution in a solar simulator

Wavelength range [nm]	Acceptance criteria [%]
0-400	0-8
400-700	30-60
700-1000	15-40
1000-2500	15-45

If the collector is equipped with a spectrally selective absorber or covering, it should be checked used to determine the influence of spectral difference on $(\tau\alpha)$ product collector. If the effective value of $(\tau\alpha)$ is under the simulator and optical air if the mass solar radiation spectrum of 1.5 differs by $\pm 1\%$ or more, it should be corrected applied to test results. Measuring the spectral quality of the solar simulator the wavelength should be within the wavelength range of $0.3 \mu m$ to $3 \mu m$ and in the plane of the collector, and should be determined with a bandwidth of $0.1 \mu m$ or less.

In order to verify this requirement, a pyrgeometer can be used to measure heat radiation. Perform several measurements on the same plane of the collector, then the value must be calculated to meet the standard requirements. This measurement is enough to perform every time the bulb is changed or whenever changes are made in the simulator or its environment.

In order to minimize the influence of heat radiation, the sky is usually very cold double glazing, cold air circulates through the double glazing to make the glass temperature close to room temperature.

3.4 Quasi-dynamic test

In the quasi-dynamic approach, the first term of Equation24 is divided into two parts, the zero-loss efficiency for beam radiation and the one for diffuse radiation.

Furthermore, the wind dependence is modelled by two correction terms added to Equation24. One term gives the effect on the zero-loss efficiency $(-c_6 u G)$. This is significant for some plastic and rubber collectors. The other term models the wind influence on heat losses $(-c_3 u (t_m - t_a))$.

After the addition of the ling-wave ‘‘thermal’’ irradiance E_L dependence of the heat losses, the collector model is complete and the full collector model for the useful output power of the collector is written as

$$Q = F'(\tau\alpha)_{en}k_{\theta b}(\theta)G_b + F'(\tau\alpha)_{en}k_{\theta d}(\theta)G_d - c_6uG - c_1(t_m - t_a)^2 - c_2(t_m - t_a) - c_3u(t_m - t_a) + c_4(E_L - \sigma T_a^4) - c_5 \frac{dt_m}{dt} \quad \text{Equation 13}$$

The basic model of incident angle dependence is made by the equation

$$k_{\theta b}(\theta) = 1 - b_0 \left(\frac{1}{\cos(\theta_i) - 1} \right) \quad \text{Equation 14}$$

as described in e.g. ASHRAE 93-77.

For collectors with special incident angle dependence, $k_{\theta b}(\theta)$ can not be described by a simple equation. Then, other options are available in extended MLR method.

In an ICS collector (integral collector storage), the residence time of the fluid in the collectors is often much longer than recommended averaging time 5-10 min. Therefore, the inlet and outlet temperatures will not reflect internal energy collector content and exact capacity correction is not possible with simplified capacity term proposed here. With a more extensive the capacitance correction term can solve this.

The quasi-dynamic test method recorded in section 6.3 of the EN 12975-2 test standard is applicable to glass collectors using liquid transport fluid. It is based on the outdoor steady-state test recorded in sections 6.1 and 6.2 of the EN 12975-2 test standard, which uses the second-order correlation between efficiency and temperature difference. The main difference with the steady-state test method is that the useful energy gain of the collector is measured in a small-time interval (5-10 minutes) that allows changes in solar irradiance and ambient temperature. All the remaining operation parameters are controlled to within a specified range listed in Table 3.

The recommended test sequence includes 4-5 days of data collection, but the actual duration of the test will depend on the weather conditions during the test. Test "Day Type " (DT) is defined as a different combination of average license plate temperature and weather conditions. The EN 12975 standard requires that each type of inlet temperature should be fixed to meet the average fluid temperature requirements defined in Table 4

The test for Day Type 1 and 2 could be completed in less than one day, however, those for Day Type 3 normally require two days. The choice of the hottest temperature T_{hot} is provided in Table 2

Table 2: Highest fluid outlet temperature as a function of collector type

Collector type	T_{hot} (°C)
Domestic hot water preparation	$T_a + 60$
District heating	$T_a + 70$
Swimming pools	$T_a + 15$
Process heating	$T_a + 90$

The standard requires the measurements specified in Table 5 to be performed during testing. Time-dependent measurement on the bottom from Table 5 must be taken with a sampling frequency of 1-6 s, and then averaged over the range of 5-10 min.

Table 3: Test condition

Collector orientation (°)	Facing south ± 5
Tilt angle (°)	45 ± 5
Solar radiation (w/m^2)	>300
Wind speed (m/s)	1-4
Mass flow rate ($Kg/s m^2$)	$0.02 \pm 1\%$

Table 4: Mean fluid temperature and weather condition per day type

Mean fluid temperature	Clear sky	Partly cloudy
$T_a \pm 3K$	Day Type 1	Day Type 2
$(T_a + T_{hot})/3$	Day Type 3	Day Type 3
$2(T_a + T_{hot})/3$	Day Type 3	Day Type 3
T_{hot} (see Table 3)	Day Type 4	Day Type 4

Table 5: Required variable measurements

Aperture, absorber and gross collector area
Fluid capacity
Azimuth and tilt angle
Global and diffuse irradiance at collector aperture
Incident long wave radiation at collector aperture
Incident angle of direct solar radiation
Surrounding air speed
Surrounding air temperature
Inlet and outlet temperature of the heat transfer fluid
Flow rate of the heat transfer fluid

The collected data must be assessed before the collector parameter identification process is initiated to ensure it, the variability and dynamic range meet the requirements obtain the collector parameters in a statistically unbiased manner way. The evaluation procedure is delivery plots that show the expected relationships while showing sufficient range of measured variables. These plots must be included in the final test results. (Intelligetn Energy Europe, 2012)

3.5 Test period and procedure

The recommended test sequence, mounting and other test requirements, are closely connected to those widely accepted for steady-state testing of solar thermal collectors, as outlined in e.g. ISO 9806-1, ISO9806-3 and ASHRAE 93-77.

The test conditions and the permitted deviation of the measured parameters during the test for the steady-state and the quasi-dynamic test are listed in Table 7.

Table 6: Test condition and permitted deviations

Parameter	Steady-state		Quasi-dynamic	
	value	Deviation from the mean	value	Deviation from the mean
Global solar irradiance G [w/m^2]	>700	± 50	$300 < G$ < 1100	–
Incidence angle of the beam irradiance θ [°]	<20	–	–	–
Diffuse fraction G_d/G [%]	<30	–	–	–
Surrounding air temperature t_a [k]	–	± 1	–	–
Surrounding air speed u [m/s]	3 ± 1	–	–	–
Collector inlet temperature t_m [k]	–	± 0.1	–	± 1

Basically, the two methods have the same requirements for suitable test data. Therefore, the recommended test sequence will be obtained and cut out those measurement data sequences corresponding to the steady-state requirements, and regular steady-state parameters can also be performed. Recognition. However, the test database must of course contain more and appropriate information, so that it is possible to identify other collector performance parameters that are included in the collector model.

Compared to steady-state testing, the number of outdoor test days will be the same, i.e. 4-5 days (4 different inlet temperatures). But depending on the actual weather at the test site and time of year, steady-state testing may need a lot more days, as the requirement for clear sky conditions around solar noon is very strong.

However, the main difference is that the test data of this method is collected throughout the day from early morning to afternoon, rather than some instantaneous values collected within a few hours of solar noon.

By measuring during the whole day, e.g. enough information about IAM-dependence is obtained. In contradiction to steady-state testing, also variable and partly cloudy condition during the test period are prescribed, making it possible to identify, e.g. the dependence of the diffuse part of the irradiance as well as the thermal capacitance of the collector(Fischer et al., 2004)(Rojas et al., 2008).

3.6 Installation required for measurements

In order to measure the different parameters mentioned previously, some elements are required to provide accurate data for further exploitation. Those requirements are provided by the EN 12975 Standard method involving a compulsory set of essential components used for the measurement. Here is a list of those main component and their respective roles.

- The solar collector oriented carefully depending on the requirements of the test (i.e. angular position and orientation of the collector regarding the sun path) and connected to one closed-loop system.
- The temperature sensors situated at the inlet, at the outlet and three different points inside the reservoir to check the temperature of use but also next to it for measuring the ambient air temperature surrounding the collector surface.
- The flow-meter measuring the flow within the circuit.
- The pyranometers measuring the total solar irradiance, the diffuse radiation when equipped with a shadow ring but also the incident long wave radiation (for sky temperature).
- The anemometer measuring the wind velocity.

3.6.1 Data acquisition

The data-acquisition card is controlled by a properly developed interface, using the LabVIEW software, running on the PC. It consists of two parts, the first is a graphical environment with components such as displays, buttons and graphs to provide a comfortable-to-use environment for the operator of the system called the front panel, and the second is the program code, which is in the block diagram and consists of built-in virtual instruments (VI) performing

functions such as analogue channel sampling, math operations, file management, etc. Includes dials, graphs, etc. for displaying parameters. LabVIEW is programmed to detect parameter changes every second and as displayed on the screen. The screen includes a block diagram for each parameter measurement which, when the program is stopped, shows the virtual form of the cable connection and the data values at each transfer stage.

LabVIEW is very powerful when it comes to creating DAQ applications. LabVIEW includes a set of VIs that let you configure, acquire data from, and send data to DAQ devices. Often, one device can perform a variety of functions, such as analog-to-digital (A/D) conversion, digital-to-analog (D/A) conversion, digital I/O, and counter/timer operations (Manual, 2003) (Exercises, n.d.)(National Instrument Team, 2015).

NI USB-6008 device

NI USB-6008 is a simple and low-cost multifunction I/O device from National Instruments.

The device has the following specifications:

- 8 analog inputs (12 bit, 10 KS/s).
- 2 analog outputs (12 bits, 150 S/s).
- USB connection, no extra power-supply needed.
- Compatible with LabView
- NI-DAQmx driver software

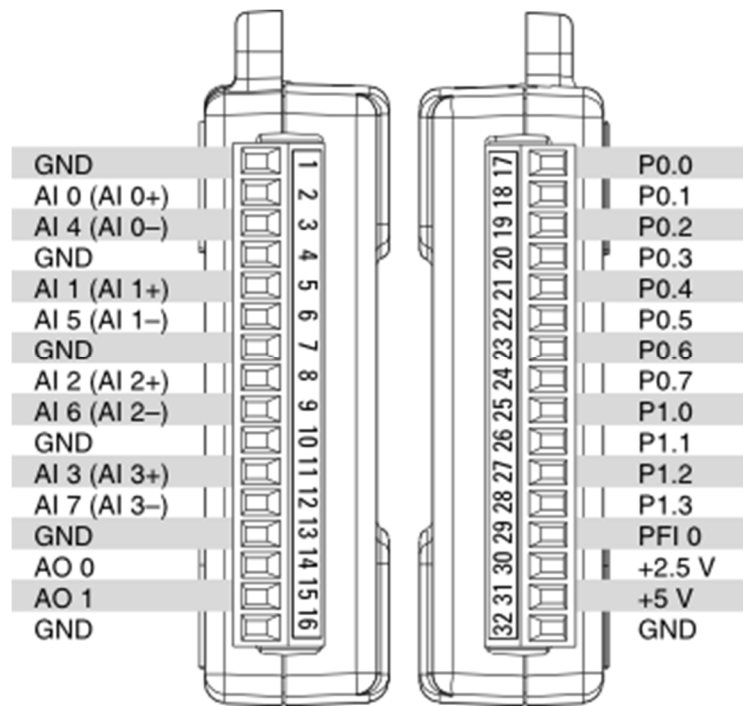


Figure 7: The appearance of NI USB-6008

NI myDAQ device:

The NI myDAQ is a low-cost portable device and DAQ shorts for data acquisition. The NI my DAQ is used to examine real world signals from electronics and sensors.

The major parts of NI myDAQ are:

- Analog input – AI
- Analog output – AO
- Digital input and output – DIO
- Audio
- Power supplies
- Digital multi meter (DMM) functions in a compact USB device

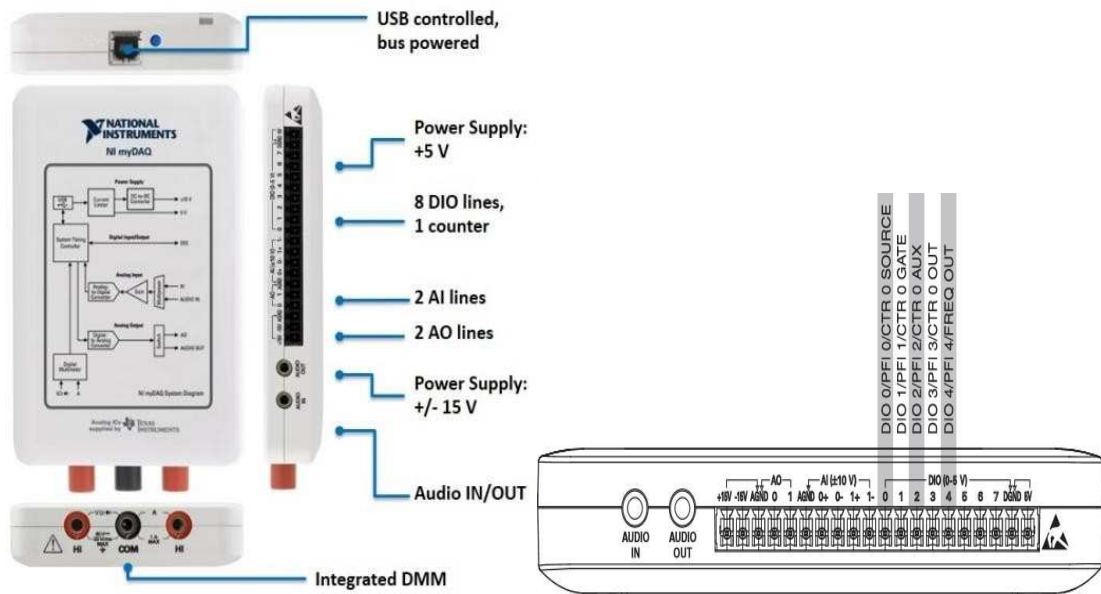


Figure 8: The appearance of NI myDAQ

3.6.2 Thermocouples

A thermocouple is a cable consisting of two wires made of two different conductors that are soldered or welded together at one end. The composition of the conductors used varies greatly and depends on the required temperature range, accuracy, span and the environment being measured. However, all types of thermocouples operate with the same basic theory: the thermoelectric effect or the Seebeck effect. Whenever a conductor experiences a temperature gradient from one end to the other, a voltage potential develops. This voltage potential arises because free electrons in the conductor diffuse at different rates, depending on the temperature. Electrons with higher energy on the hot side of the conductor diffuse faster than electrons with lower energy on the cold side. The net effect is that a charge builds up at one end of the conductor and creates a voltage potential from the hot and cold ends (Koprivica et al., 2018) (Laurila, 2017).

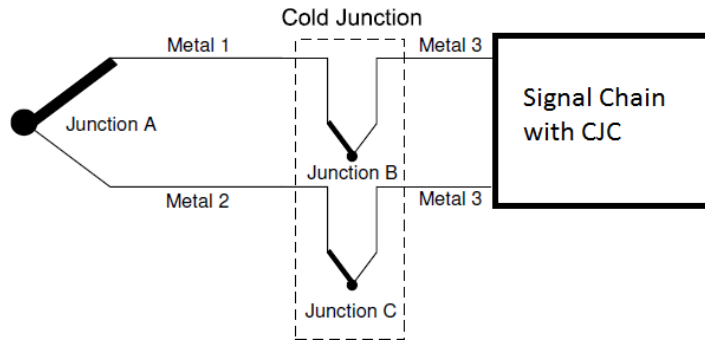


Figure 9: Thermocouple junction diagram

We can monitor thermocouples with comprehensive PC based data acquisition systems. Thermocouples have some special requirements for signal conditioning, signal conditioning extensions for instrumentation system (SCXI), are the signal conditioning front-end for plug-in data acquisition (DAQ) cards. SCXI systems are ideal for amplifying, filtering and even isolating the very low voltage levels that thermocouples generate.

3.6.2.1 Cold-junction-compensation

Thermocouples require some form of temperature reference to compensate for these unwanted parasitic thermocouples. The term cold junction comes from the traditional practice of holding this reference junction at 0°C in an ice bath (Started & Material, 2005)(Laurila, 2017)(More, 2014).

To solve the cold junction problem, there are different methods such as cold junction in ice bath which we can connect the thermocouples wires into copper wires in the ice bath and there is no thermovoltage generated in that connection, in the other hand we can fix the temperature by having a small connection box that has a temperature control keeping the box always at a certain temperature, or measure the temperature of the cold junction.

All methods mentioned above are not practical, hence, exploring a measuring device is the best solution to measure the temperature of cold junction all the time. The SCXI is a product preserved by National Instrument for signal conditioning

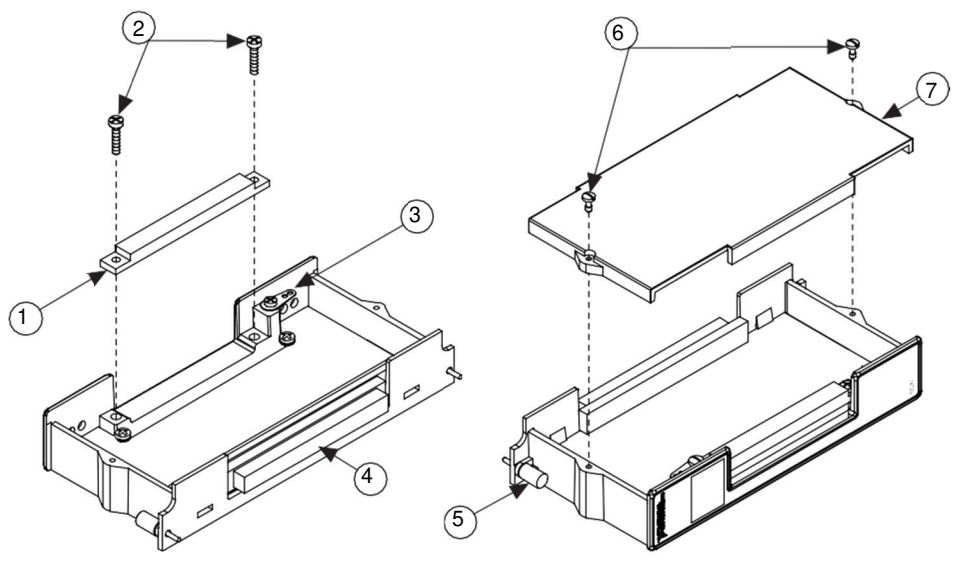
SCXI-MS100 is ideal for multi-channel temperature applications in many environments, and combines SCXI and data acquisition (DAQ) products to use thermocouples that require amplification, cold junction compensation (CJC) and high-resolution analog-to-digital conversion for precision Temperature measurement. Digital converter (ADC). In addition, the VirtualBench-Logger software included in our interface for displaying and recording data.

To set up and use our SCXI-MS100 temperature measurement system, we need the following:

- DAQ device
- SCXI-1000 chassis with AC power cord
- SCXI-1102 module
- SCXI-1303 terminal block
- SCXI-1349 cable assembly
- NI-DAQ driver software (version 6.5.1 or later)
- VirtualBench application software (version 2.5.1 or later)

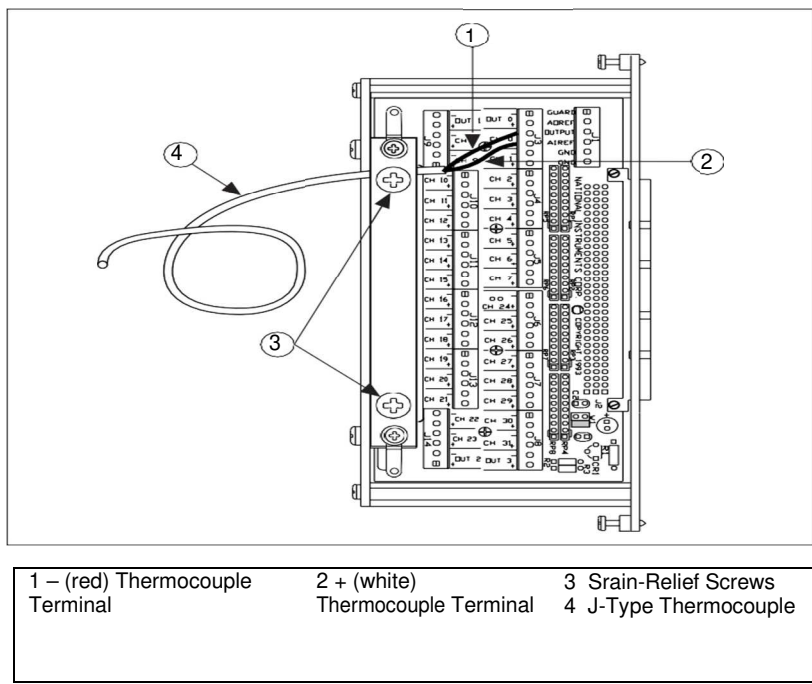
The following section detail how to install our software and hardware in our SCXI-MS100 system:

- Install the NI-DAQ driver software and the plug-in DAQ device.
- Install the VirtuaBench-Logger.
- Install the SCXI hardware components. This procedure includes how to set up our SCXI chassis, install SCXI modules, attach terminal block and cables, configure our SCXI chassis using Measurement & Automation Explorer.
- Connect the thermocouples to the SCXI-1303 terminal block.



1 Strain-Relief Bar	3 Earth Ground	4 Mating Connector	6 Top Cover Screws
2 Strain-Relief Screws	Solder Lug	5 Thumbscrew	7 Top Cover

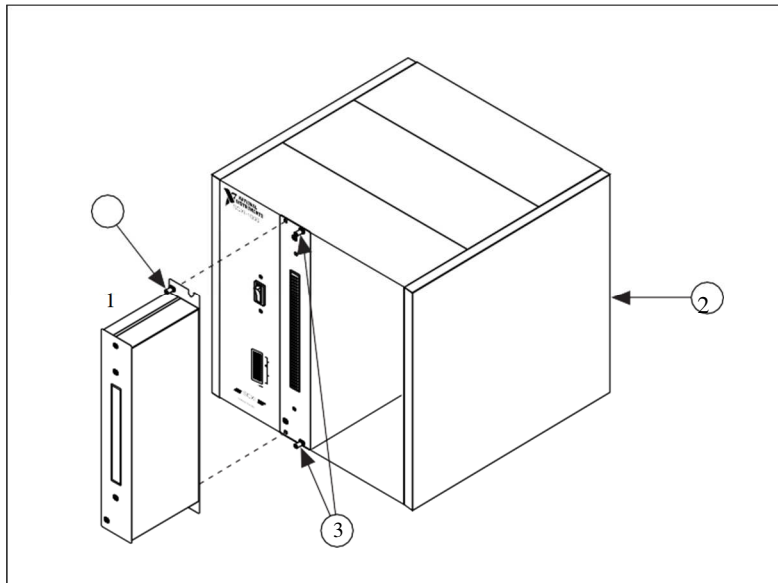
Figure 10: SCXI-1303 parts locator diagram



1 – (red) Thermocouple Terminal	2 + (white) Thermocouple Terminal	3 Strain-Relief Screws	4 J-Type Thermocouple
---------------------------------	-----------------------------------	------------------------	-----------------------

Figure 11: Thermocouple connected to channel 0 of the SCXI-1303 Terminal Block

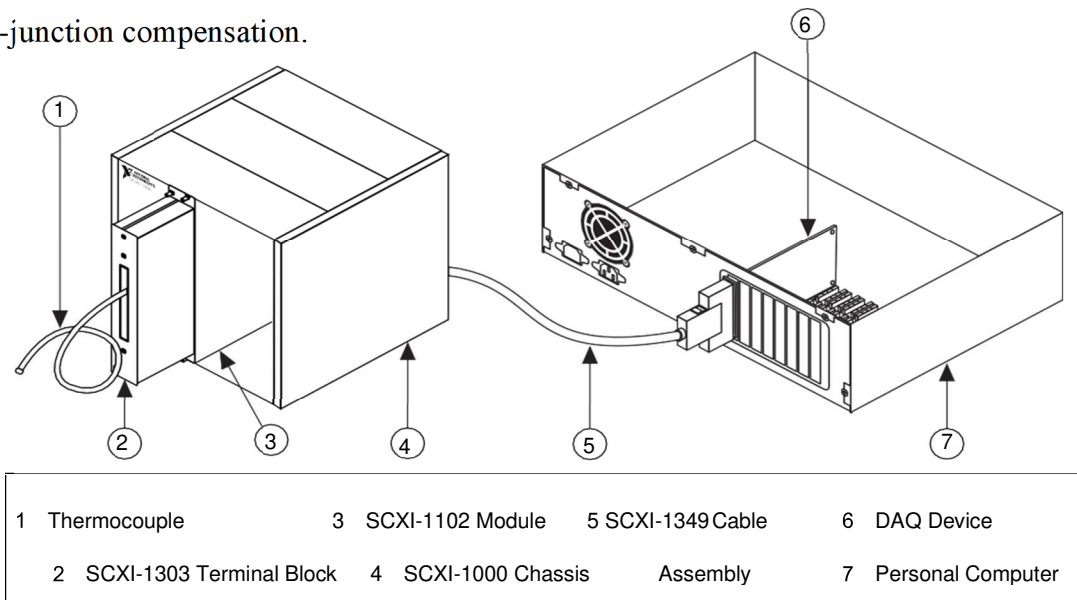
- Connect the SCXI-1303 to our SCXI-1102 Module



1 Terminal Block Thumbscrew	2 Chassis	3 Module Thumbscrews
--------------------------------	-----------	----------------------

Figure 12: Connecting the SCXI-1303 Terminal Block to the SCXI-1102 Module

Place the SCXI chassis away from any extreme temperature differential to minimize the temperature gradient inside the terminal block and maintain its isothermal nature for accurate cold-junction compensation.

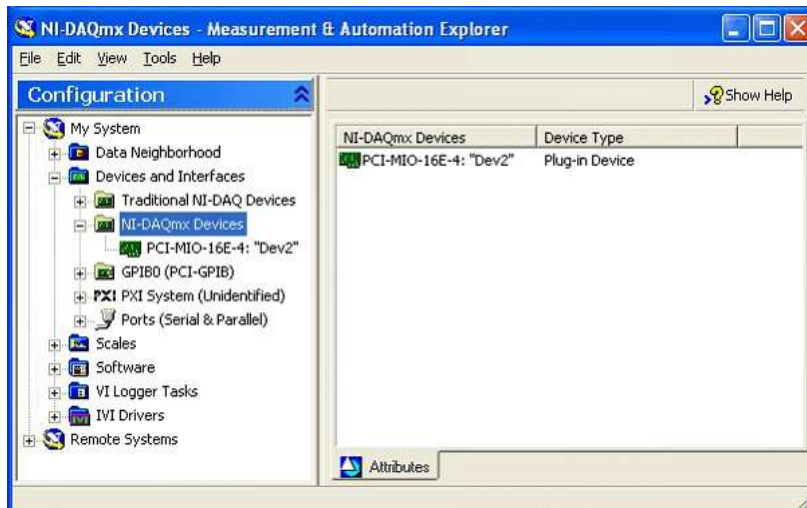


1 Thermocouple	3 SCXI-1102 Module	5 SCXI-1349 Cable	6 DAQ Device
2 SCXI-1303 Terminal Block	4 SCXI-1000 Chassis Assembly	7 Personal Computer	

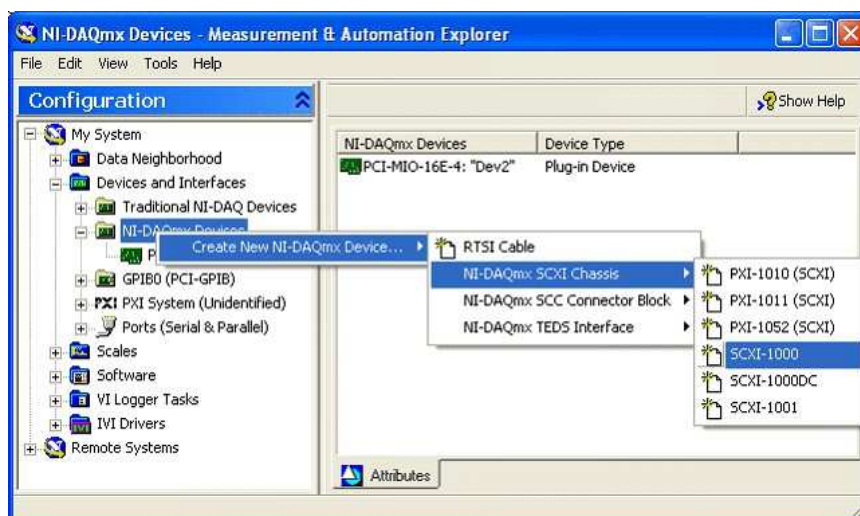
Figure 13: Complete installation

To configure our system software, we should make sure we have installed NI-DAQ software

- Launch Measurement & Automation Explorer.
- Expand “Devices and Interfaces” under “My System”.
- Expand “NI-DAQmx Devices” and check to make sure you see your installed DAQ card.



- Right -click on the “NI-DAQmx Devices” folder under “Devices and Interfaces”
- Choose Create new NI-DAQmx Device and continue on to your specific signal

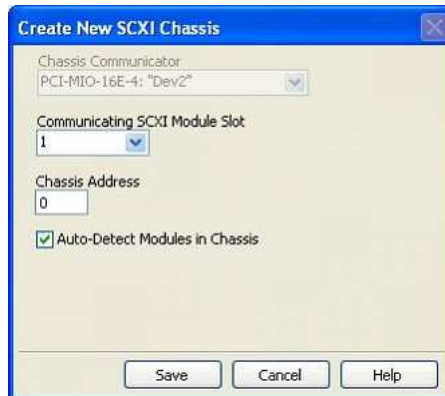


conditioning device (SCXI-1000 shown).

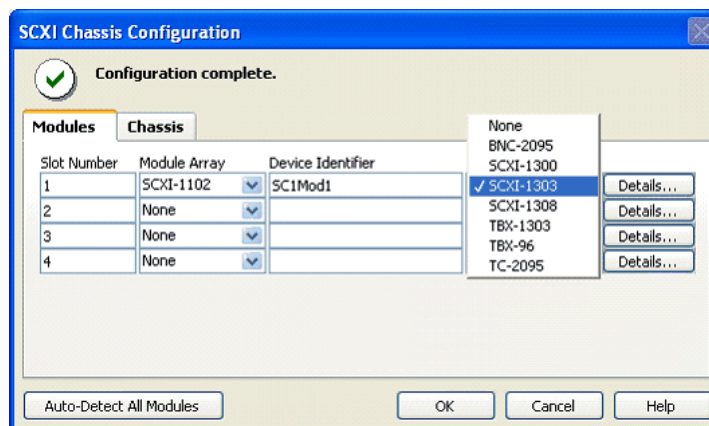
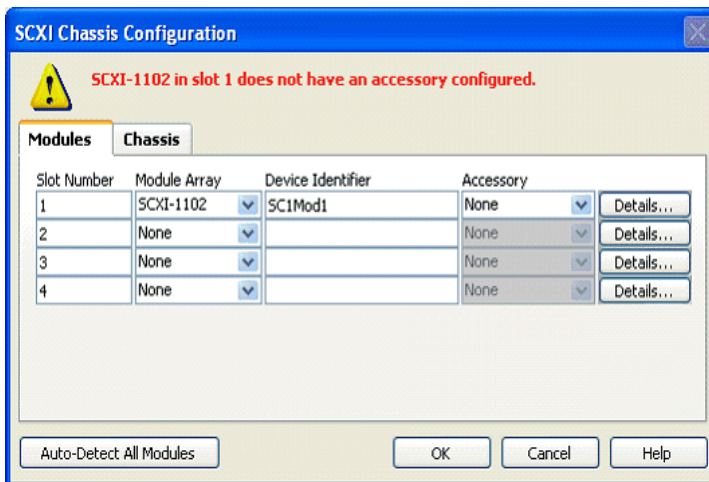
- Create new SCXI chassis

The "chassis communicator" is the DAQ card to which our chassis is cabled.

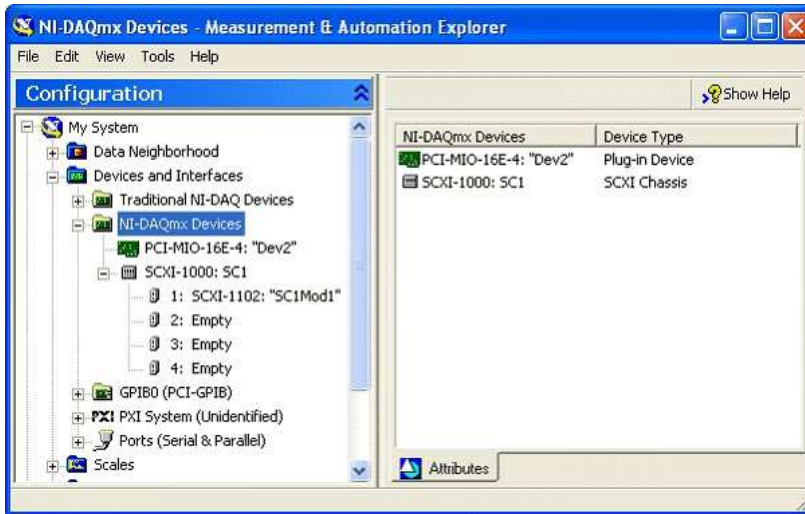
The "communicating module slot" is the slot in which we have the cabled module.



- Our modules should auto-detect (chassis must be powered on), accessories will not auto-detect: select an accessory for each module.



- Our device will now appear under “NI-DAQmx Devices”



Configure VirtualBench-Logger

Run the VirtualBench-Logger software, located under: **Start>>Programs>>National Instruments VirtualBench>>VirtualBench-Logger**

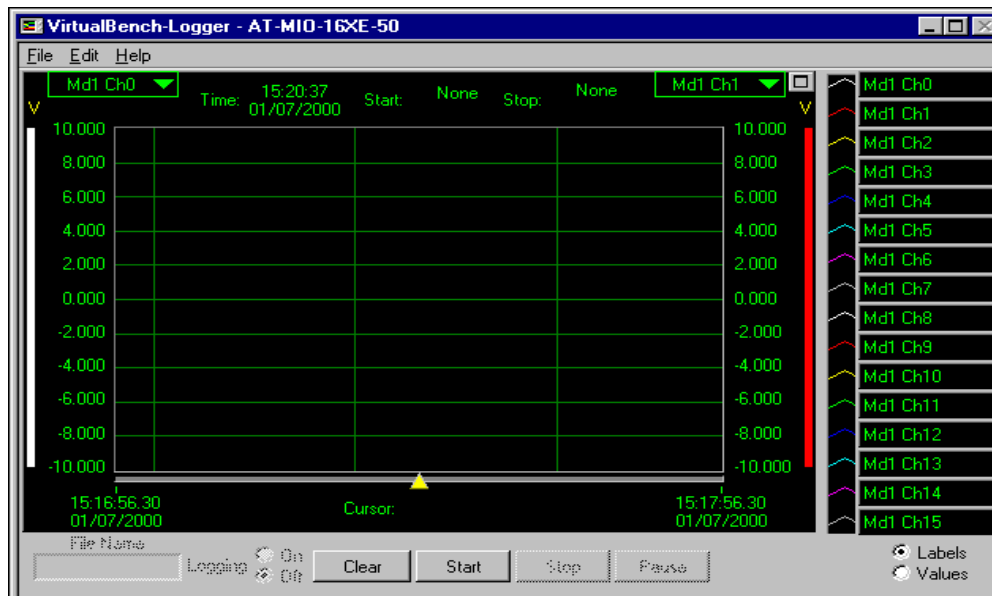


Figure 14: VirtualBench-Logger Main Run-Time Window

To configure the settings in the VirtualBench-Logger select **Edit>>Settings**

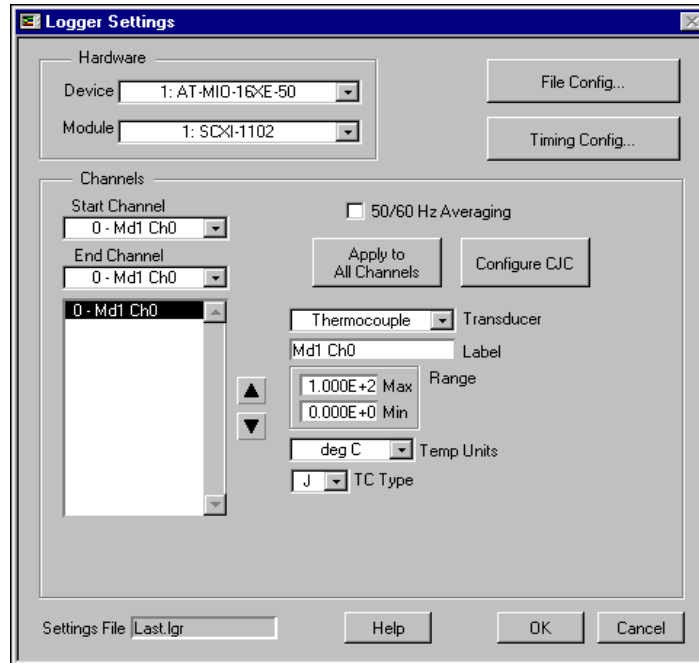


Figure 15: VirtualBench-Logger Setting Window

To configure our CJC source:

- Set the **Cold Junction Compensation Source** to **CJTEMP**.
- Set the **Cold Junction Compensation Source Type** to **Thermistor**.

We are now ready to collect temperature data. Press the **Start** button on the main run-time window, the **VirtualBench-Logger** window displays temperature data from the thermocouple.

Up to this point, this installation guide has explained how to use only one channel. To connect and measure more thermocouples, the factory-default SCXI-MS100 system accommodates up to 32 channels performed in the following steps:

- Remove the SCXI-1303 terminal block. Refer to connect the thermocouples and connect the SCXI-1303 to our SCXI-1102.
- Run the VirtualBench-Logger software and go to **Edit>>Settings**. Modify the **Start Channel** and **End Channel** to reflect the number of thermocouples.

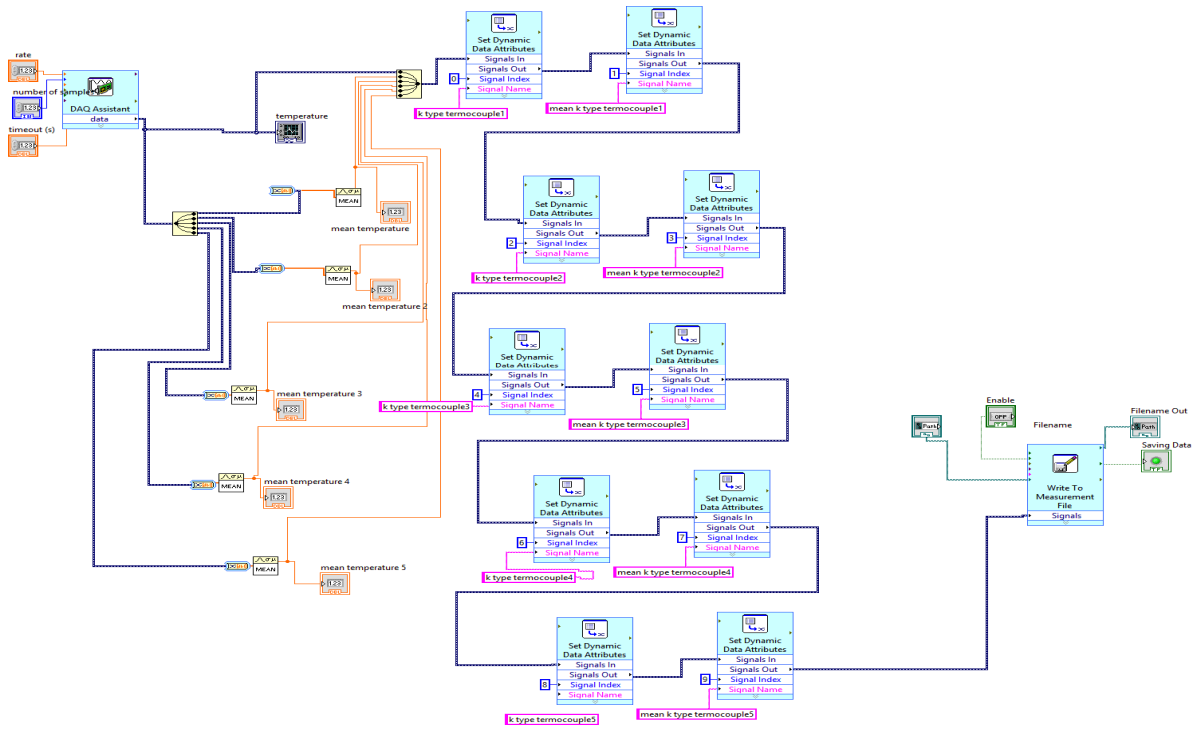


Figure 16: Block diagram of thermocouple type k

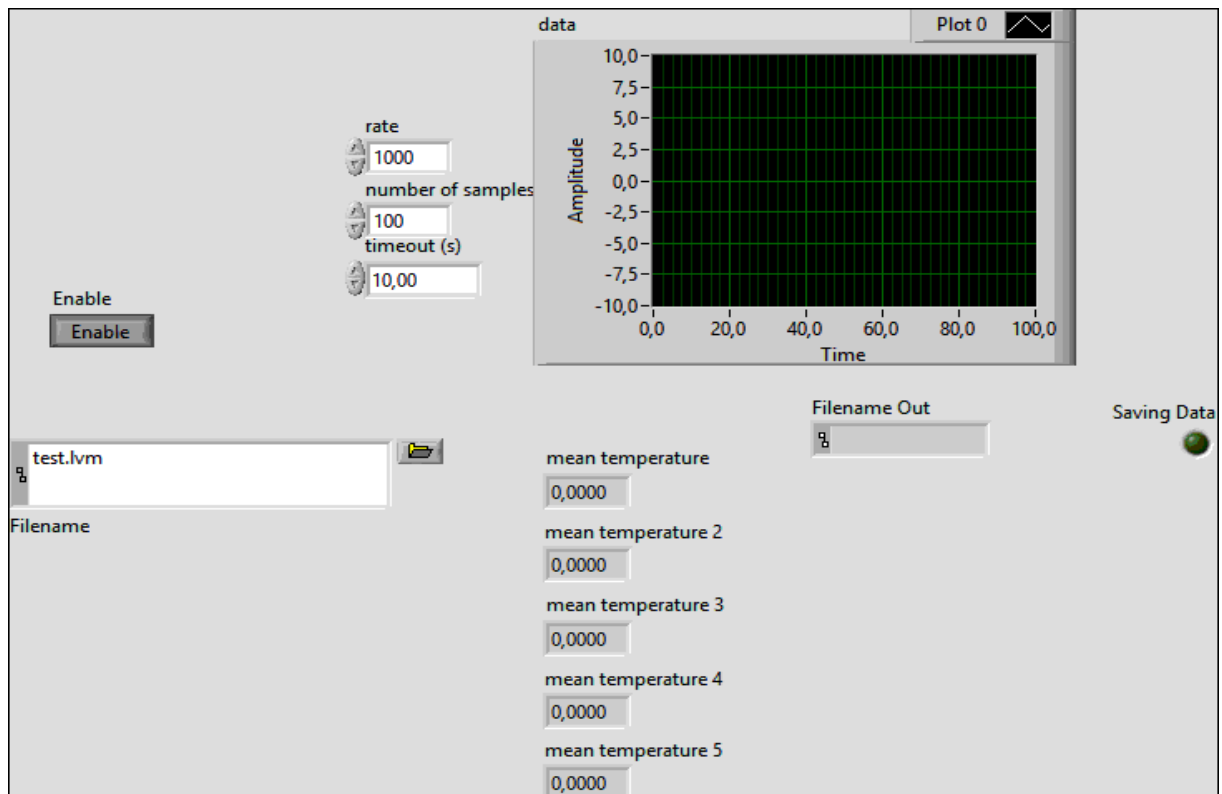


Figure 17: Front panel thermocouple type k

3.6.3 Ambient temperature

The LM35 succession are precision united circuit temperature strategies with a voltage of output directly proportional to centigrade temperature.

LM35 sensor consist of 3 pins, pin 1 is connects to Vcc for power supply from the NI myDAQ +15, pin 2 is connects to the analog pin A0 and the third pin is connecting to the ground of the NI myDAQ.

The characteristics are:

- Measurable range is -55°C to 150°C .
- Linear with 0.5° certified accuracy at $+25^{\circ}$.
- + Vs used is 15V
- The production at 36°C is 0.36V and the production at 21°C is 0.21V.

The input of analog data of DAQ is managed and standardized to display the accurate temperature by multiplying the DAQ assistant production with a numeric constant '100'. When the temperature is less than 40°C , green color light will be observable in LabView front panel and red color light when the temperature more than 40°C (Peeters et al., 2010)(Psikuta et al., 2014).

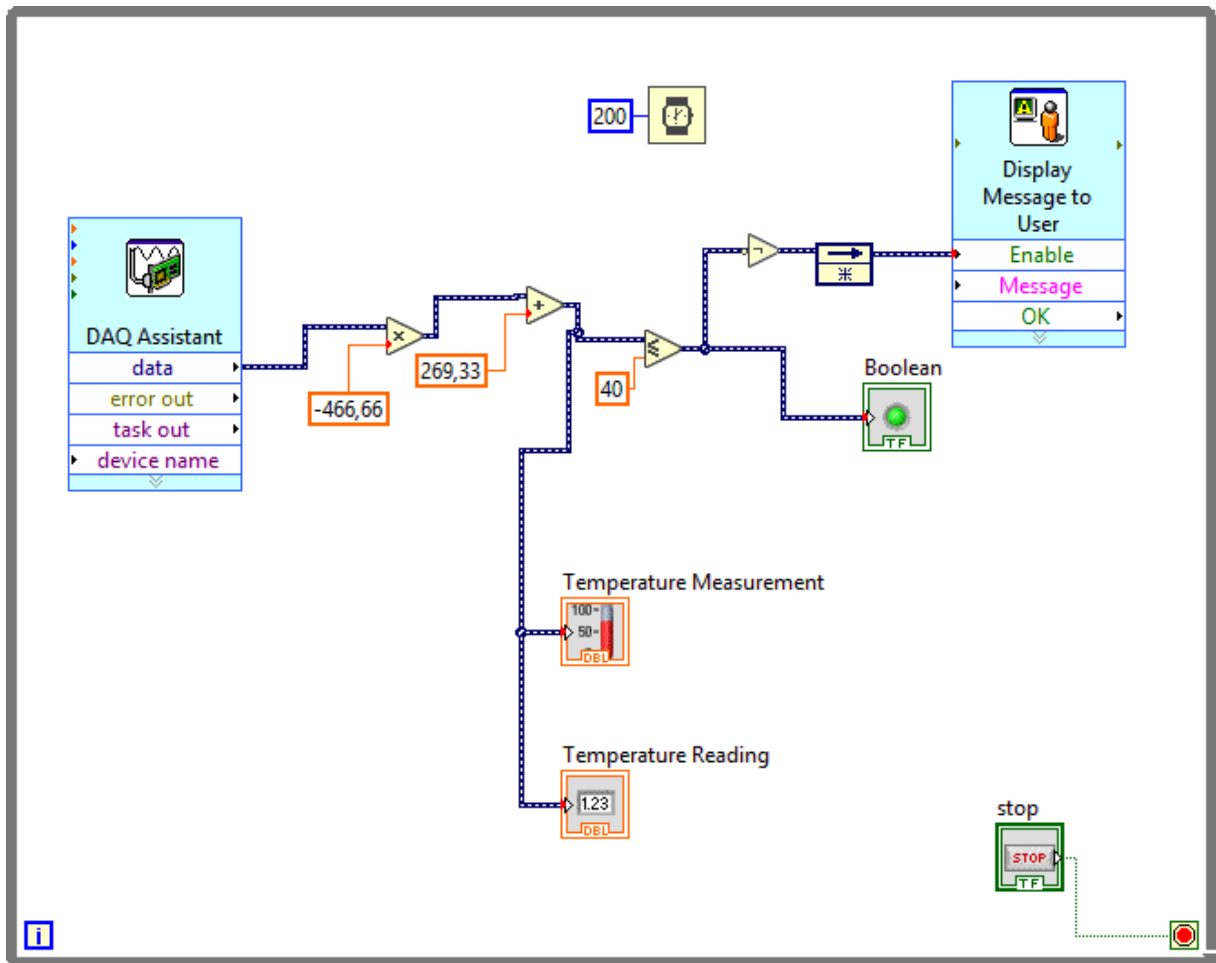


Figure 18: Block diagram of ambient temperature

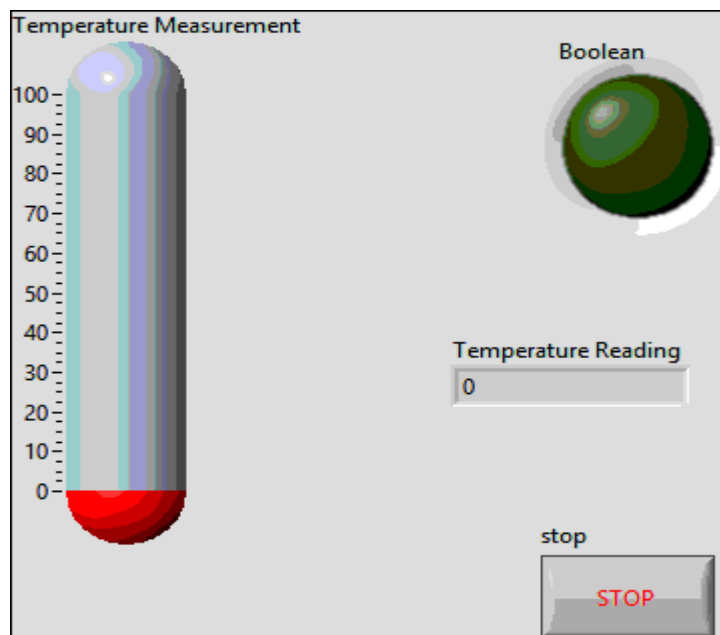


Figure 19: Front panel of ambient temperature

3.6.4 Inlet mass flow

The flow sensor is a turbine style sensor, using the rate a small fan spins to demine the speed of the fluid passing through it. The magnetic blades within the meter spin past a Hall Effect sensor generating pulses as the turbine rotates.

The created program was designed to use the signal from the flow sensor and translate that signal into a flow rate.

The SLA5800 series thermal mass flow meters and mass flow controllers have gained broad acceptance as the standard for accuracy, stability and reliability (Sheet et al., 2014).

REQUIREMENTS

- NI DAQ device with analog inputs and outputs. **NI USB-6008**
- SLA Series MFC analog device.
- Power supply for MFC.
- DB15 to WE cable (p/n: S124Z361AAA).

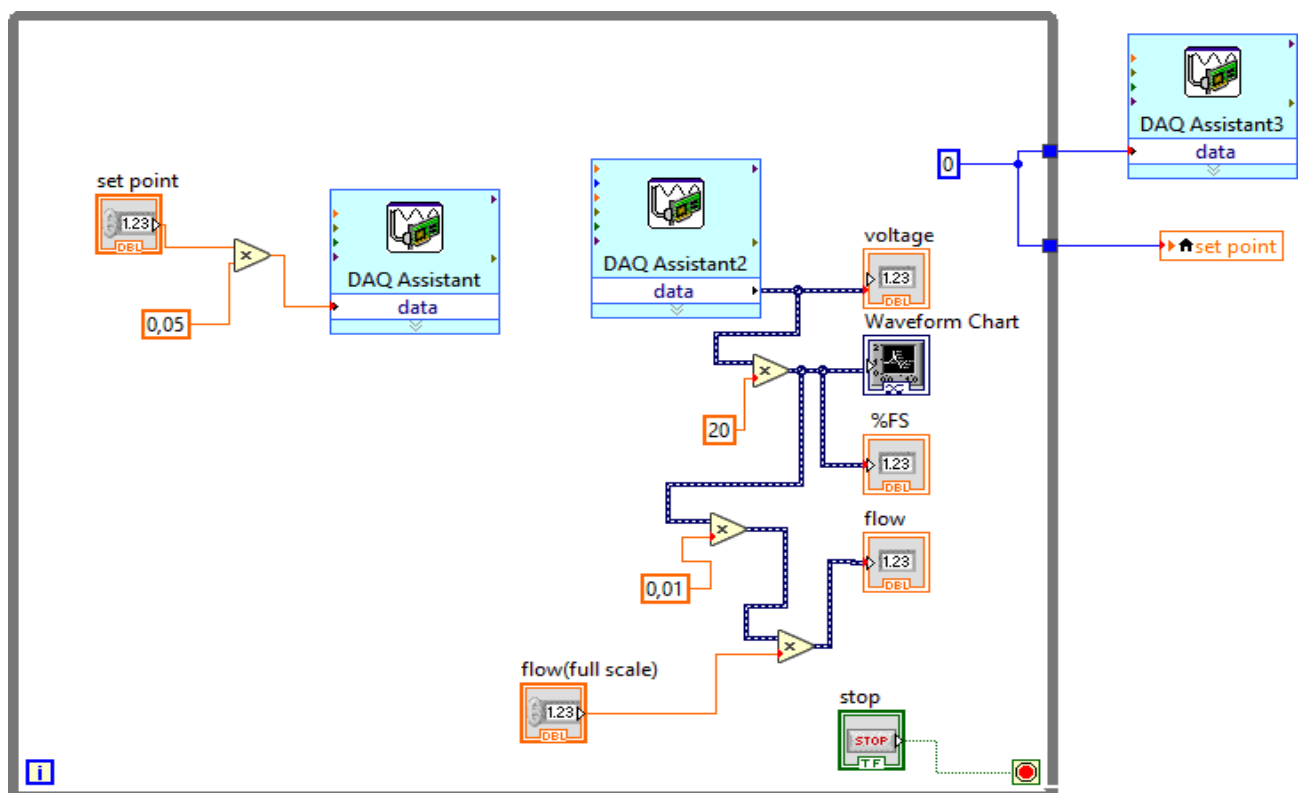


Figure 20: Block diagram of flow meter SLA5800

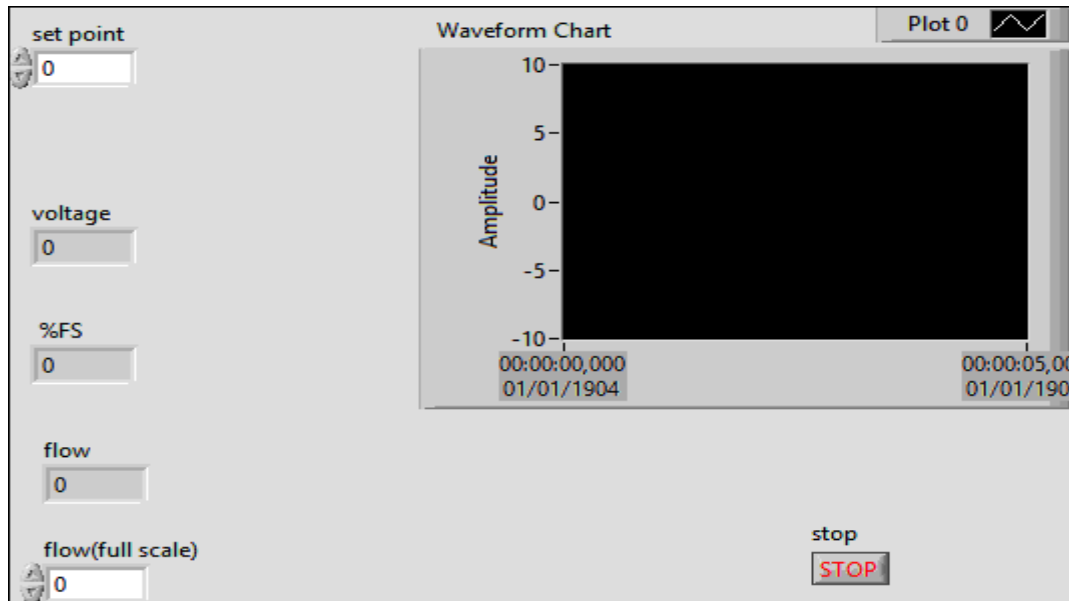


Figure 21: Front panel of flow meter SLA5800

3.6.5 Surrounding air speed

The vernier anemometer is an impeller type device that has its axis of rotation parallel with the wind. The wind causes the impeller, shaft, and magnet to rotate producing an electrical signal whose frequency is proportional to the wind speed. The calibration of the anemometer is done by using the slope intercept formula ($y = mx + b$), where m is the slope, and b is the y-intercept. The two calibrated wind speeds used in this lab consist of m/s and Km/h. For m/s the slope equals to 10m/s/V, and the y-intercept equals to -10 m/s. For Km/h, the slope equals to 36 Km/h/V, and the y-intercept equals -36 Km/h. These formulas were typed into LabVIEW formula nodes (Figure22), where x in the formula was the analog input signal read from the anemometer. However, a vernier adapter was needed to plug the meter into the myDAQ module. The adapter made it easy for the analog signal from the anemometer to be read into the myDAQ module.

The front panel Figure23 consists of three green LEDs; one for each of the three possible wind speed ranges of high, normal, and low. A red LED to signify an alarm for a high wind speed condition. This alarm also has an alarm string that will output the statement high wind when this condition is met. Also, in the front panel is a chart that will read in the analog signal as it happens live. In addition to the chart, there are also real time speed reading that change with the current wind speed values. There is a speedometer type meter that acts as if there is

an analog measuring device present, and another scale to show the high wind speed condition. Lastly, a stop pushbutton is in the top left corner of the front panel to stop the live reading of wind from the anemometer. (Thepnurat et al., 2018) (Chinomi et al., 2017)

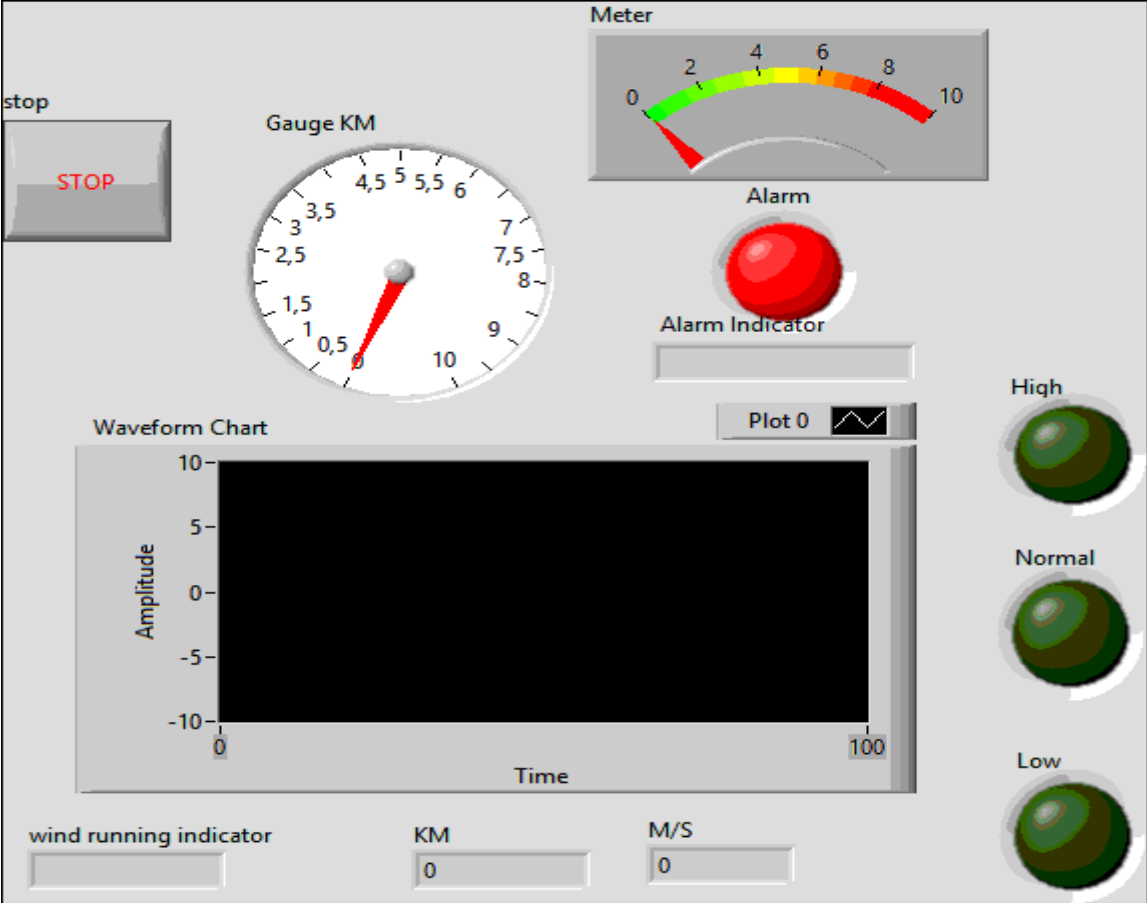


Figure 22: Front panel of surrounding air speed

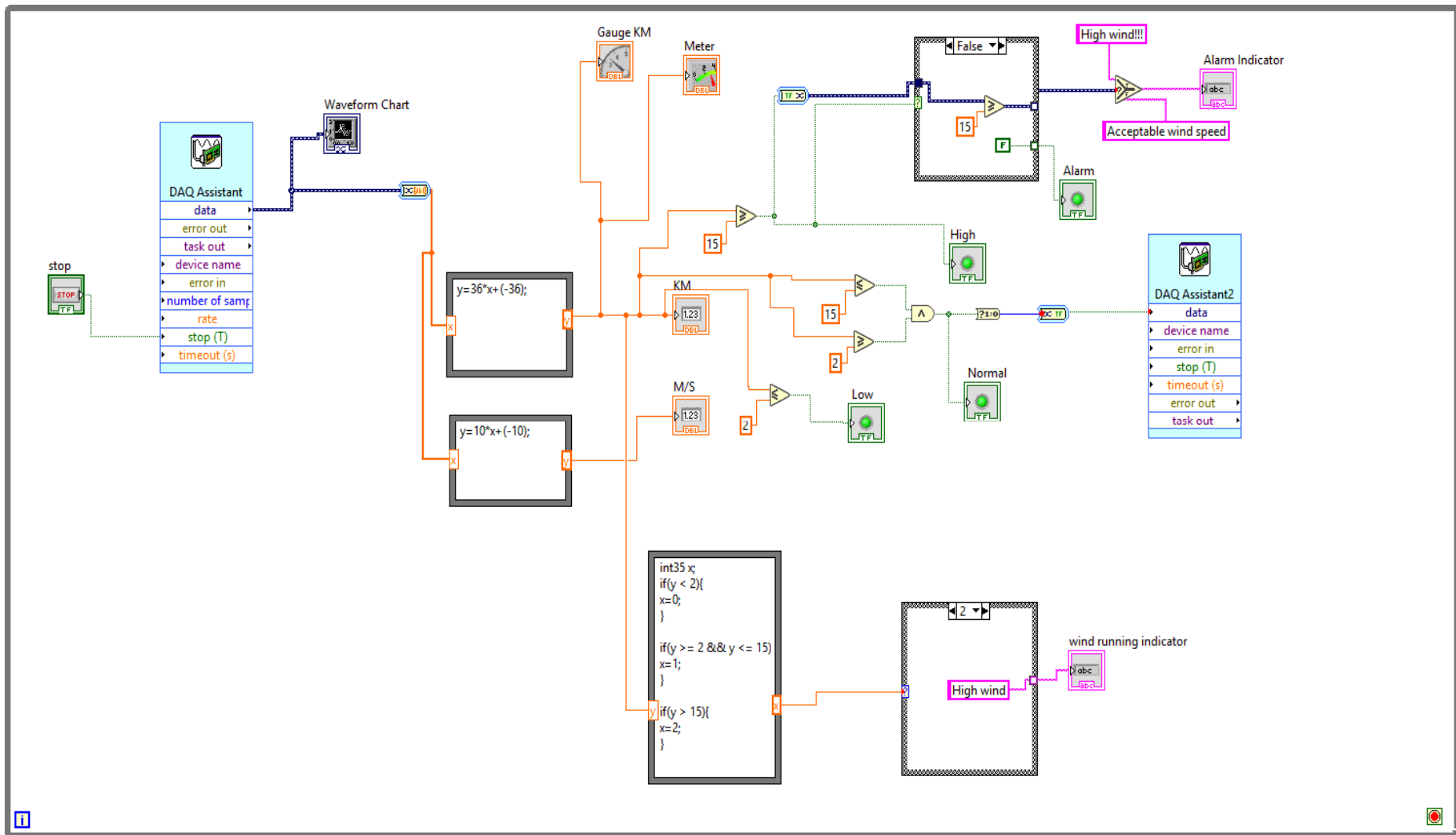


Figure 23: Block Diagram of surrounding air speed

3.6.6 Surrounding air temperature

Air temperature is a key parameter in many precision metering fields. The temperature of the air itself is critical. In other cases, the air temperature is used to control and infer the temperature of the metered product, such as size standards and weight. However, even if the balance is maintained under good laboratory conditions, the temperature of the thermometer itself will usually differ by 0.1°C or more, and the difference between larger objects can be as much as one-tenth of a degree. For precision measurement, this level of error is very important.

It is well known that temperature sensors are affected by optical and infrared radiation, and this effect may be difficult to detect. However, it is generally believed that the size of the error caused by a specific radiation load depends on factors such as the emissivity of the sensor surface, the sensor size, etc., which are rarely considered in the metrology literature. The reason is that in a steady state, when the thermometer reaches a stable temperature, the radiant heating or cooling is balanced by the air flow around the sensor

The choice of sensor and sensor size depends on the specific application, but possible options include platinum resistance thermometers (PRT), thermistors, thermocouples and fiber optic thermometers.

However, as the diameter of the PRT decreases, self-heating generally becomes more important, and it may be necessary to reduce the measurement current to achieve an acceptable little self-heating. The thermistor can be as small as a millimeter in diameter and provides excellent sensitivity in a small temperature range. However, the self-heating of the thermistor is more important than the small diameter PRT.

For Reducing the test current requirements in PRTs and thermistors may make the use of thermocouples competitive with RTDs. The diameter of the thermocouple can be as small as 0.025 mm and has no self-heating function. Hybrid technology using thermocouples, where the temperature of the reference junction is stabilized in a metal block, and SPRT capsules are used for measurement with low uncertainty.

The block diagram and the front panel in Figure24 and Figure25 respectively represent thermocouple configuration to collect the average of surrounding air temperature and save data in the block (write to measurement file)(De Podesta et al., 2018).

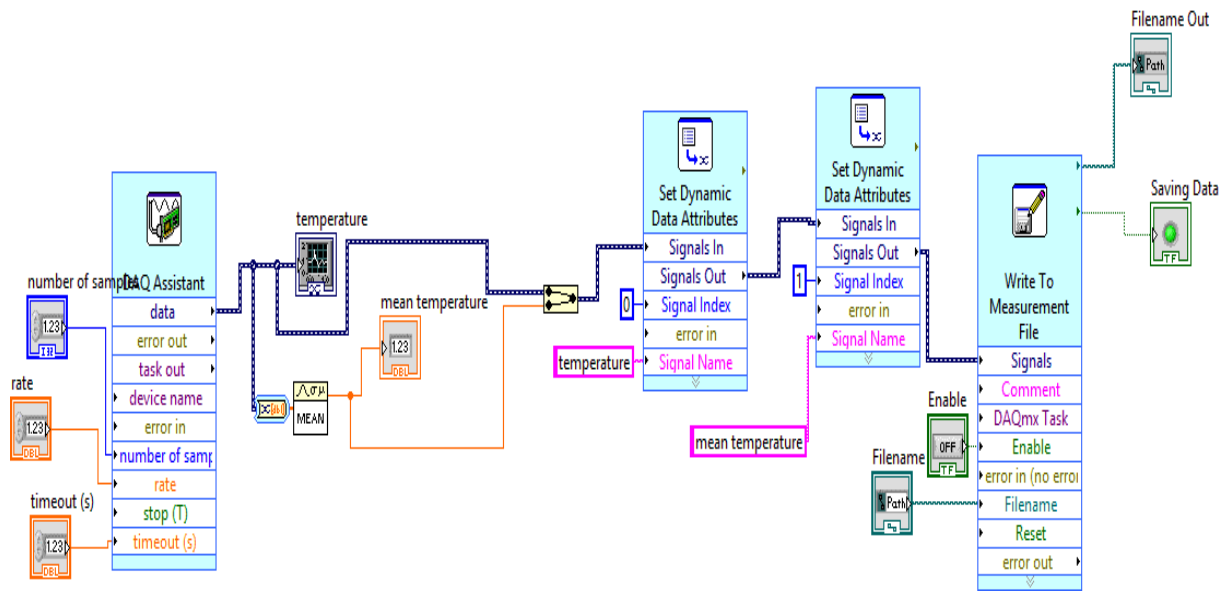


Figure 24: Block diagram of surrounding air temperature

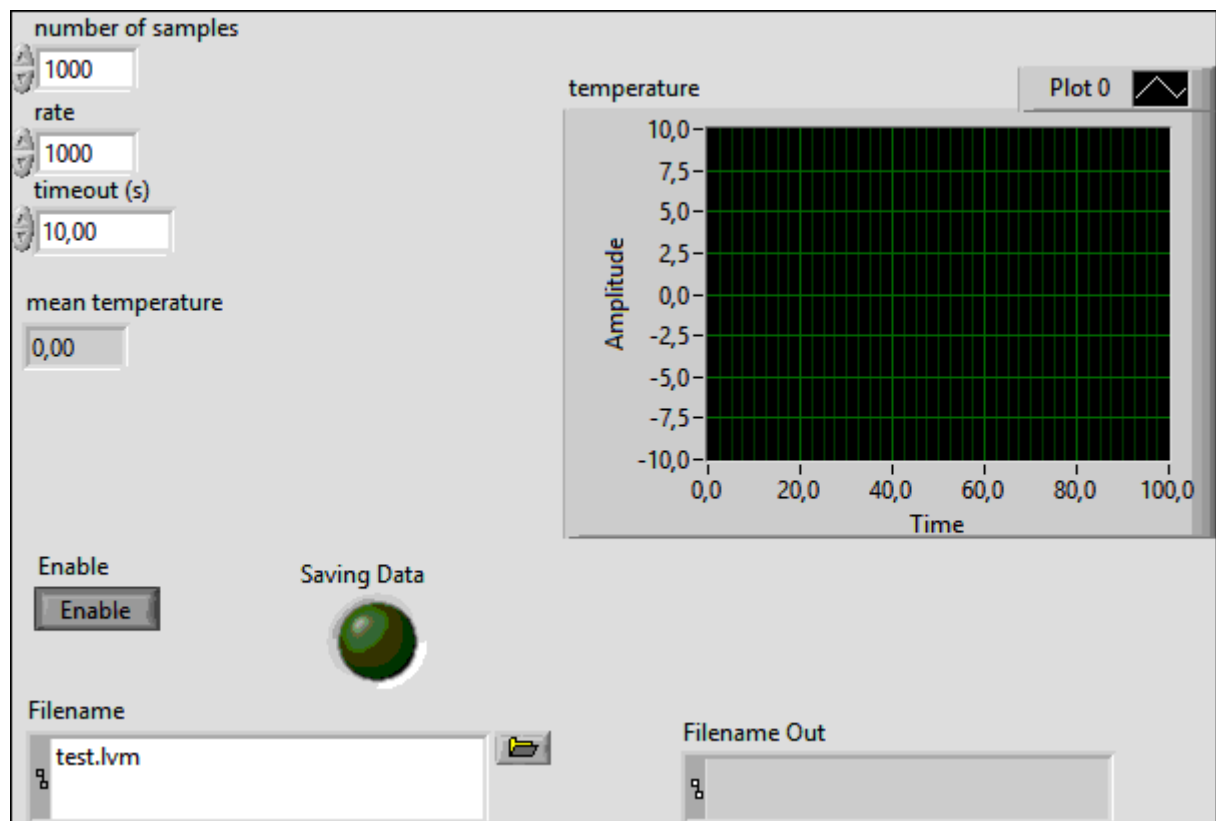


Figure 25: Front panel of surrounding air temperature

3.6.7 Azimuth and tilt angle

The direction of the planar solar collector can be varied in tilt and azimuth directions to maximize incident radiation. One way to accurately assess the solar energy available on an inclined plane and determine the best angle to orient a fixed-angle panel is to place the pyranometer in several plane directions and record the total irradiance for a sufficiently long period of time.

In practice this is rarely completed, so models to predict the tilted irradiance are used. There are two concepts fundamental to the method described.

First, the cloud's optical properties from satellite searches are included in radiative transfer (RT) calculations. Second, the inclined irradiance is derived from the surface field of radiance. RT methods are often used to model the intensity of solar radiation under a clear sky. Sometimes cloud effects are introduced as a correction to the cloudless sky value depending on the cloud albedo coming from the satellite or adjusted based on the observed historical ground level irradiance.

The irradiance on a tilted plane angled at tilt β and azimuth γ is a combination of the downwards and upwards radiance fields such that the bounds of the integration is over the hemisphere with base in the plane of the solar collector:

$$I_T = \int_0^{2\pi} \int_0^{\theta_m} L(\theta, \phi) \cos\theta_d \sin\theta \, d\theta \, d\phi \quad \text{Equation 15}$$

Where the angle between the normal of the tilted plane and the radiance direction of interest is given by

$$\cos\theta_d = \cos\beta \cos\theta + \sin\beta \sin\theta \cos(\phi - \gamma) \quad \text{Equation 16}$$

And the bound of the integration θ_m is in the plane of the solar collector such that

$$\theta_m = \frac{\pi}{2} - \tan^{-1}(\cos(\phi - \gamma) \tan\beta) \quad \text{Equation 17}$$

The radiance field L is calculated at a resolution of 3° in the polar direction and 10° in the azimuthal direction using the DISORT radiative transfer code (Stamnes et al.,2000), as part of the libRadtran package (Mayer and Kylling,2005), with pseudo spherical correction to

improve accuracy at low solar elevations (Dahlback and Stamnes,1991). θ is the polar angle and z is the azimuthal angle (Cerón-Bretón et al., 2011).

3.6.8 Incident angle of direct radiation

The amount of the solar radiation incident on a surface is inversely proportional to the value of incidence angle which is defined as the angle between the solar rays and the normal line on the surface. The incidence angle can be calculated by a long equation which depends on several angles (Hafez et al., 2017) (Kocer et al., 2015) (Cerón-Bretón et al., 2011).

The sun position with respect to an observer on earth can be fully described by means of two astronomical angles, the solar altitude α and the azimuth z . The following is a description of each angle.

Declination angle δ : the angle between the sun's direction and the equatorial plane. δ varies smoothly from $+23.45^\circ$ at midsummer in the northern hemisphere to -23.45° at northern midwinter.

$$\delta = 23.45^\circ \sin \left[\frac{360}{365} (n + 284) \right] \quad \text{Equation 18}$$

Where n is the day in the year($n = 1$ on 1 January)

- Hour angle h is the angle through which the Earth has rotated since solar noon. Since the Earth rotates at $360^\circ/24 \text{ hour} = 15^\circ/\text{h}$. The hour angle is positive in the evening and negative in the morning.

$$h = (\text{local time} - 12)15^\circ \quad \text{Equation 19}$$

- Solar altitude angle α : the angle between the solar beam and the horizontal.
- Solar zenith angle ϕ : the angle between the solar beam and the normal on the horizon.

Solar altitude and solar azimuth angles are complementing ($\alpha + \phi = 90^\circ$)

$$\sin \alpha = \cos \phi = \sin L \sin \delta + \cos L \cos \delta \cos h \quad \text{Equation 20}$$

Where L is the local latitude, values north of the equator are positive and those south are negative.

- Solar azimuth angle z : the angle between the solar beam and the longitude meridian.

$$\sin z = \cos \delta \sinh / \cos \alpha \quad \text{Equation 21}$$

These angles calculated based on a specified mounting and orientation of the solar collector.

- Tilt angle β is the angle between the plane surface and the horizontal.
- Surface azimuth angle Z_s is the angle between the normal to the surface and the local longitude meridian.
- Angle of incidence θ is the angle between solar beam and surface normal.

$$\cos \theta = \sin L \sin \delta \cos \beta - \cos L \sin \delta \sin \beta \cos Z_s + \cos L \cos \delta \cos \beta \cosh + \sin L \cos \delta \cosh \sin \beta \cos Z_s + \cos \delta \sinh \sin \beta \sin Z_s \quad \text{Equation 22}$$

```

day=input('Day=');%insert the sequence of the day in the month, from 1 to 31

x=input('Month=');%insert the corresponding number of the month, from 1 to 12

m=[0 31 59 90 120 151 181 212 243 273 304 334];

n=m(x)+day %this step evaluate the day sequence number in the year

declination_angle=23.45*sin(360*(284+n)/365*pi/180) %see equ(1)

d=declination_angle*pi/180;

hour=input('Hour =');%insert the hour in the 24 hour system (e.g. 13 for 1 p.m.)

min=input('Minute=');%insert the minute, from 0 to 59

hour_angle=((hour+min/60)-12)*15 %see equ(2)

min=input('Minute=');%insert the minute, from 0 to 59

hour_angle=((hour+min/60)-12)*15 %see equ(2)

h=hour_angle*pi/180;

B=input('Slope(tilt angle)in deg=')*pi/180;

```

```

L=input('Local latitude in deg=')*pi/180;

Z=input('Surface azimuth angle in deg=')*pi/180;

%the values above is local and independent.

Daily_optimum_tilt_angle=(L-d)*180/pi

Altitude_angle= asin(sin(L)*sin(d)+cos(L)*cos(d)*cos(h))*180/pi %see equ(3)

a=Altitude_angle*pi/180;

Solar_zenith_angle=90-Altitude_angle

phi=Solar_zenith_angle*pi/180;

Solar_azimuth_angle=asin(cos(d)*sin(h)/cos(a))*180/pi %see equ(4)

z=Solar_azimuth_angle*pi/180;

Incidence_angle=acos(sin(L)*sin(d)*cos(B)-
cos(L)*sin(d)*sin(B)*cos(Z)+cos(L)*cos(d)*cos(h)*cos(B)+sin(L)*cos(d)*cos(h)*sin(B)
*cos(Z)+cos(d)*sin(h)*sin(B)*sin(Z))*180/pi %see equ(5)

theta=Incidence_angle*pi/180;

Gbn=input('Solar radiation on horizontal plane =');

RB=cos(theta)/cos(phi) %see equ(6)

Solar_radiation_on_the_surface=RB*Gbn%see equ(7)

```

Figure 26: Matlab code of incident angle of direct radiation

3.6.9 Global, direct and diffuse irradiance

The measurement and control of the solar irradiance of the solar collector are important because of the characteristic test of the solar cell will be needed to adjust the accuracy of the flux. Many techniques were applied to achieve that. One common approach has been to have two sensors, one measuring radiation from the whole sky (global irradiance), the other measuring the whole sky apart from the sun (diffuse irradiance). The shading is generally done using a shade ring, adjusted to match the track of the sun across the sky for that day.

This approach requires accurate alignment to the Earth's axis, and frequent adjustment. In practice, the problems of alignment and frequent adjustment make this a difficult and sometimes unreliable measurement to make.

Another approach has been to use an array of pyranometers, with different fixed orientation, and thus different views of the sun and sky. The known position of the sun combined with the sensor orientation is used to solve for values of global and diffuse from the differing sensor output.

A pyranometer is the main instrument used to measure the global solar irradiance (radiation). It measures the sun's energy from all directions in the hemisphere in the plane above the instrument. A proper pyranometer use a flat plate covered with thermopiles that absorbs sunlight and produces a voltage proportional to the temperature.

The global horizontal irradiance can be split up into two components, the direct irradiance (the beam from the sun), and the diffuse irradiance.

the global horizontal irradiance I_g is equal to:

$$I_g = I_b \cos Z + I_d \quad \text{Equation 23}$$

Where I_b is the beam irradiance, I_d is the diffuse and z is the angle of incidence.

A pyranometer stationed on ground level for the purpose of measuring the beam irradiance, must first measure the global and diffuse components, usually done by two separate instruments, and divide the difference by $\cos z$ (Baltazar et al., 2014)(Zaaiman, 2012).

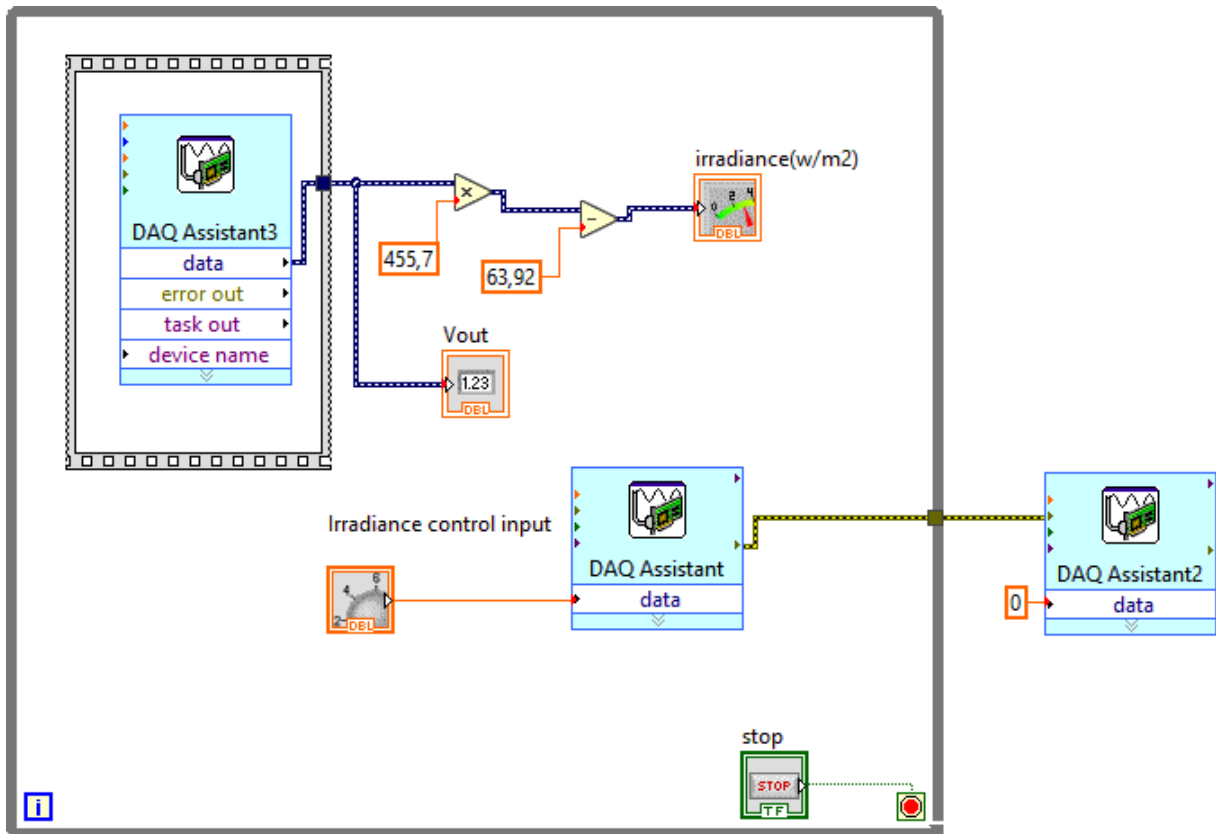


Figure 27: Block diagram of the pyranometer

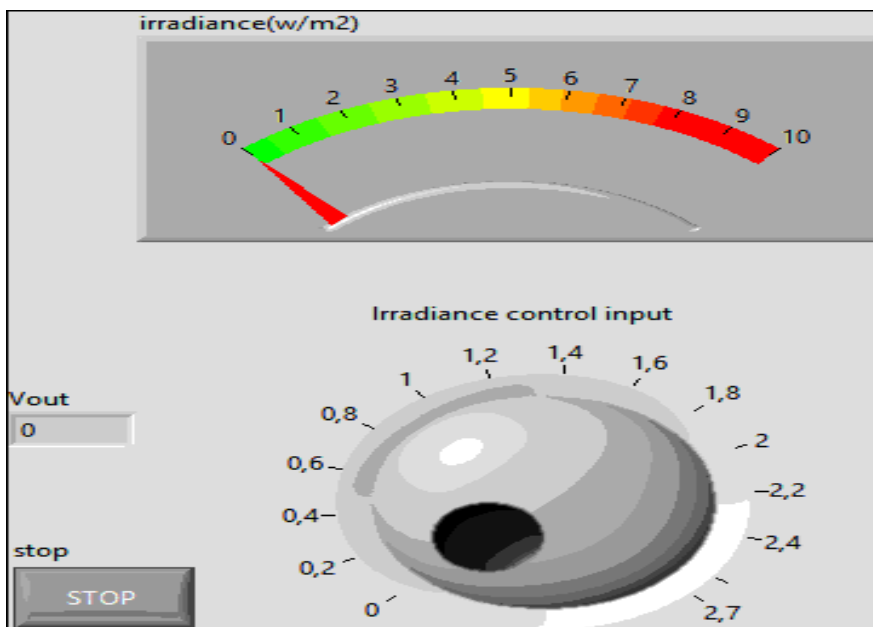


Figure 28: Front panel of the pyranometer

3.6.10 Incident longwave radiation

The surface temperature is locally controlled by the surface energy balance, that is, the balance between the net surface radiation and the turbulence of heat and moisture. These terms have great geographic, seasonal, and diurnal variations. Net radiation consists of solar radiation absorbed by the surface minus the difference between upward and downward longwave radiation.

$$R_n = S_d - S_u + L_d - L_u = \lambda E + H + G \quad \text{Equation 24}$$

Where R_n is the surface net radiation, S_d is the surface incident solar radiation, S_u is the surface reflected solar radiation, L_d is atmospheric downward longwave radiation, L_u is the surface emitted longwave radiation, λE is the latent heat flux, H is the sensible heat flux, and G is the heat storage in the ground. Of these terms, L_d is the most fundamental for understanding the impact of increasing CO_2 and other greenhouse gases on climate but is also considered to be the most poorly quantified from observations.

Rather than estimate L_d as that needed to balance measurements of the other terms in Equation 20, a more direct method is to obtain it from observations of other atmospheric quantities as input to its calculations based on radiative transfer. Of particular importance for this calculation is the vertical distribution of atmospheric water vapor, temperature and clouds. This method uses two different frameworks to provide the required "re-analysis" of atmospheric properties, which introduces uncertainty because they only use modeled cloud or satellite observations, which may also be subject to inaccuracy. The estimated limit of cloud cover.

The most direct measurement approach is with the use of pyrgeometers. Such measurements have been made through some internationally coordinated monitoring activities, such as the World Climate Research Program (WCRP), Baseline Surface Radiation Network (BSRN), the Global Energy and Water Cycle Experiment (GEWEX), Coordinated Energy and water cycle Observations Project (CEOP) and the FLUXNET. These networks have provided long-term continuous measurements of L_d for nearly 20 years at globally distributed sites, in particular at the BSRN sites. The instrument used to directly measure L_d is called a pyrgeometer. It has a body, a thermopile, and a dome filter that blocks out solar shortwave radiation (America, 2003)(Hill, 1976)

3.7 Weather station

Weather station data such as air temperature, wind speed, and solar irradiation are required for simulation. The parameters from the weather station can be read directly from the server.

The weather station system contains the control module, weather MicroServer, the network router, LAN (SQL server express and LabVIEW), and cloud database are related to the data storage.

3.7.1 Capricorn 2000EX weather station

The Capricorn 2000EX weather station contains the control module and sensors. The control module includes a data storage marked with data and time. In addition, the max/min information is stored at user-defined intervals. The dual onboard RS-232 interfaces allow connection to a display console, modem, or directly to a computer at the same time.

3.7.2 The weather MicroServer

The weather MicroServer is an independent proprietary system using the Linux operating system. The server produces an “internet ready” weather monitoring system by automatically providing FTP output, XML web service, and Internet browser user interface. With the weather MicroServer, data logging is a possibility. It can be connected to a network using an Ethernet cable. It also provides real-time weather data. This gives the user the possibility to monitor the weather at any computer connected to the network.

3.8 Data collection from the weather station

In order to collect data from the weather station, the data reading system should be connected to the ethernet connection to have the accessibility to the given IP-Address. Having connected to the ethernet connection and providing the necessary authentication, the real-time data can be read from the global website.

For collecting data from the weather station, the reader needs to be connected to the server for every single reading. This makes collecting data a challenging task for every collection. However, by automating the data collection using the LabVIEW ModBus library, the system automatically collects data every time that the receiver got connected to the server.

3.8.1 Developing the application to save weather station data

In order to have communication from the server with the program, the communication can be executed by the ModBus protocol.

The ModBus protocol uses master and slave architecture. The master transmits a request to a slave and the slave responds. This gives the master full control over the information. This request is a layered set of data, where the application data unit (ADU) is the first layer. TCP/IP, ASCII, and remote terminal unit (RTU) are the three types of ADUs.

The MicroServer weather station works with ModBus TCP mode for making the request and reading data from the sensor. In this sense, the LabVIEW has library called ModBus capable of requesting reading data from the server.

The reading system as the client, or the master, requests the server to read the data and the server gives the client the request data. With the LabVIEW application, it can be done to write a program based on the master TCP client with the given IP address and requesting the registered input value for each sensor. The data which are read unjustified raw 16-bit figured which have to be converted to the right amount with the offset and factor for every parameter.

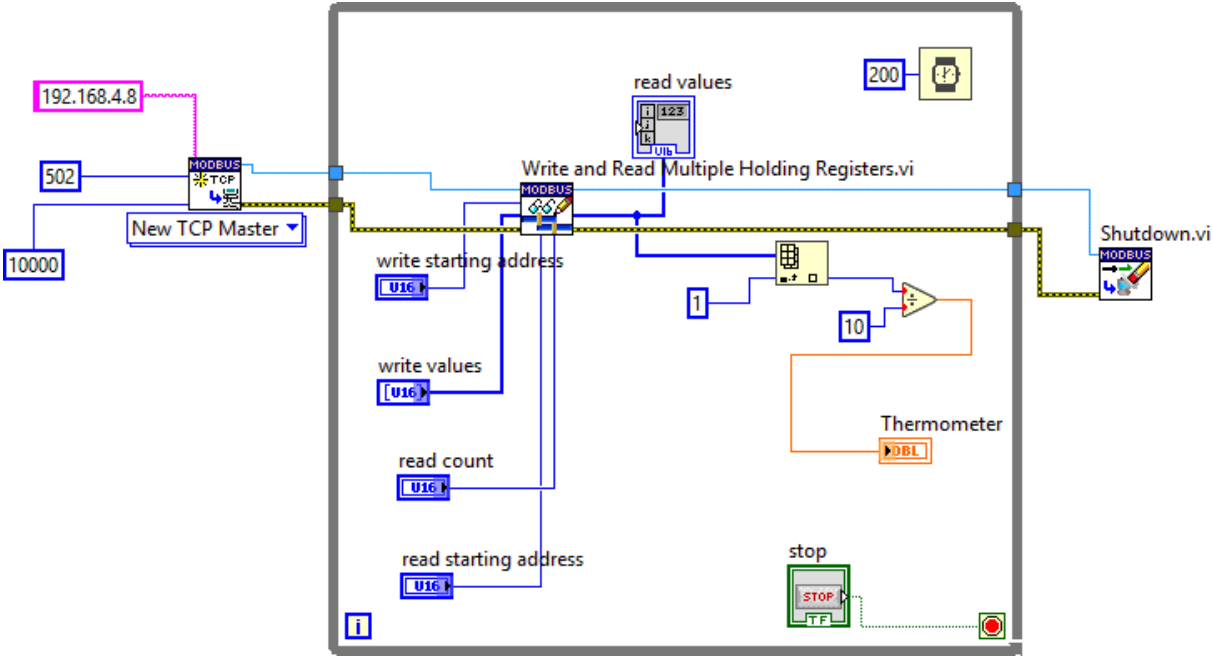


Figure 29: Bloc diagram for the weather station data

In this application, first, a TCP master box is created in to get access to the local host, then the IP address of the host is given. As it is given from the manual and the weather station resources, the IP address for the weather station to get access via the ethernet connection in the university is 000.000.0.0 with the port number of 502. A reading application from the ModBus library is created to read data. In this icon, the input registry of each section and sensor needs to be addressed. However, all data that are going to be read are in the form of 16- or 32-bit unjustified numbers which give the client different values from those in the real-time. The unjustified data will be converted to the real data which corresponds to the exact number of temperature other parameters.

$$\text{Parameter value} = (\text{unsigned 16-bit integer} + \text{offset}) / \text{factor} \quad \text{Equation 25}$$

In the weather station system, every offset and factor for each factor is given and it needs to be put in the application in order to get the real data from the server.

For example, for the temperature the offset is (-17920) and the factor is 256. Consequently, for a data which the unjustified number is equal to 27080, the real value for the temperature with the equation would be approximately 35.78°F. After the conversion from Fahrenheit to Celsius, the temperature is 2.1°C, which is correspond to the real value of the day it was recorded.

The next thing for the storing data is automatic data storing. In this sense, a program needs to be developed to get the data every day automatically. An application needs to be developed corresponds to the main program which collect the data from LabView every time with or without using the application at the time. Finally, all measured data will be stored in a database created in the SQL server to collect all of them in one table.

After storing measured data in the database, the final step is to save them in a cloud storage. The main advantage of storing data in a virtualized database, namely cloud storage, is feasibility if getting access to that information for everyone via different locations or using multiple computers(Khan, 2012)(Susmitha & Sowya Bala, 2014).

4 Discussion

4.1 sensors

Transducers can be used to detect a wide range of different physical phenomena such as movement, electrical signals, radiant energy, and thermal, magnetic, or mechanical energy. They are used to convert one kind of energy into another kind. The type of input or output of the transducer used depends on the type of signal detected or process controlled; in other ways, we can define a transducer as a device that converts one physical phenomena into another one.

There are many different types of transducers; each transducer has input and output characteristics.

Sensors produce in output a voltage or current signal according to the variation of physical phenomena that are measuring. There are two types of sensors: active and passive. Active sensors require external power supply to work; instead, passive sensors generate a signal in output without external power supply.

4.2 DAQ hardware

DAQ system can be defined as a set of electronic systems, which any of the following functions:

- The input: processing and conversion to digital format using ADCs. The data are then transferred to a computer for display, storage, and analysis.
- The processing: conversion to analog format, using DACs. The analog control signals are used for controlling a system or process.
- The input of digital signals, which contain information from a system or process.
- The output of digital control signals.

The sensor is usually an integrated circuit (IC) Output very small DC voltage, DC current Or AC signals in response to physical changes Quantity. The signal is usually small and must Usually amplified, filtered or otherwise adjusted Before applying to measuring

instruments. Hence, we need signal conditioning to accurate the most suitable measurements.

4.3 Signal conditioning

Signal conditioning is a vital function in the data acquisition process. This can be accomplished through different hardware modules, for example the SCXI provided by National Instruments.

Signal conditioning circuits are used to process the output signal from sensors by the application of filtering, isolation, amplification, linearization or error compensation to eliminate the errors coming from the transformation of the physical phenomena to signal.

In addition, as presented in section 4.3.2 we choose to use thermocouples for his characteristics such as measuring very high temperature, robust, cheap and without excitation but in the other hand when the connection point of the wires is taken into different temperatures there will be a thermo-electric current generated called Seebeck effect which we need to eliminate with cold junction compensation.

4.3.1 Sensor cables:

The electrical signal from the sensor entering the data acquisition system may contain harmful noise. Because the digital signal has discrete characteristics, it is relatively anti-interference. In contrast, analog signals are directly affected by relatively low levels of interference. The main noise transmission mechanisms include capacitive coupling and inductive coupling. One way to reduce errors due to capacitive coupling is to use shielded cables and place conductive materials between the signal cable and the source of interference.

4.3.2 Digital isolation:

The electrical module is used to obtain the digital input signal and at the same time disconnect the current connection between the signal source and the measuring device. These modules not only isolate, but also convert the input to a standard voltage level, which can be read by data acquisition equipment.

4.3.3 Analogue isolation:

The analog isolation module is used to protect the equipment from contact with high voltage, disconnect the ground loop and eliminate large common-mode signals. Three types of analog isolation are widely used: low-cost capacitive coupling or "flying capacitor", optical coupling with good performance and moderate cost, and high isolation and precise but high-cost transformer coupling.

4.3.4 Low-pass filtering:

The filter is used to separate the desired signal from the undesirable signal. Bad signals are noise, rising AC line frequency, radio or television interference, and signal frequencies higher than half of the sampling frequency. Usually, low-pass filters are used to control these unwanted error sources, excluding the part of the spectrum where the desired signal is not present.

4.3.5 Amplifiers:

The amplitude of the analog sensor signal can vary within a wide range. However, analog-to-digital (A/D) converters require high-level signals to perform optimally. In many cases, amplifier modules are used to boost possible low-level signals to the desired amplitude. The amplifier module is also used to standardize the voltage output of all sensors to a common voltage, such as 0-5 DC voltage.

5 Conclusions and future work

In this thesis, a more accessible and realistic way of development of a computer-based data-acquisition system for monitoring of solar collector unit is presented. The proposed system consists of a set of transducers (sensors) for measuring meteorological parameters. The sensor signals are first filtered and amplified using precision electronic circuits and then are interfaced to a PC, using a commercially available data-acquisition cards. The collected data are further processed, displayed on the monitor and stored in the disk using the National Instruments LabVIEW software. In addition, LabVIEW provides an easy-to-use graphical environment, allowing system operators to use complex data processing algorithms to easily process the collected data without having to understand the design of the data acquisition system in detail.

6 References

- America, S. (2003). Instruction Manual Instruction Manual. *International Business*, 1–183.
- Baltazar, J. C., Sun, Y., & Haberl, J. (2014). Improved methodology to measure normal incident solar radiation with a multi-pyranometer array. *Energy Procedia*, 57, 1211–1219. <https://doi.org/10.1016/j.egypro.2014.10.109>
- Cerón-Bretón, J. G., Cerón-Bretón, R. M., Rangel-Marrón, M., Muriel-García, M., Cordova-Quiroz A.V., & Estrella-Cahuich, A. (2011). *International Journal of Energy and Environment*. 5(3), 328–336.
- Chinomi, N., Leelajindakrairerk, M., Boontaklang, S., & Chompoo-Inwai, C. (2017). Design and Implementation of a smart monitoring system of a modern renewable energy micro-grid system using a low-cost data acquisition system and LabVIEW™ program. *Journal of International Council on Electrical Engineering*, 7(1), 142–152. <https://doi.org/10.1080/22348972.2017.1345226>
- Cleber Pizzato Dallegrove. (2019). 2019.
- De Podesta, M., Bell, S., & Underwood, R. (2018). Air temperature sensors: Dependence of radiative errors on sensor diameter in precision metrology and meteorology. *Metrologia*, 55(2), 229–244. <https://doi.org/10.1088/1681-7575/aaaa52>
- Duffie e Beckman. (1991). Duffie, J.A., Beckman, W.A., 1991. Solar Engineering of Thermal Processes, second ed. John Wiley & Sons Inc., New York. In *American Journal of Physics*.
- Exercises, S. S. (n.d.). *Introduction to DAQ with LabVIEW*.
- Fischer, S., Heidemann, W., Müller-Steinhagen, H., Perers, B., Bergquist, P., & Hellström, B. (2004). Collector test method under quasi-dynamic conditions according to the European Standard EN 12975-2. *Solar Energy*, 76(1–3), 117–123. <https://doi.org/10.1016/j.solener.2003.07.021>
- Hafez, A. Z., Soliman, A., El-Metwally, K. A., & Ismail, I. M. (2017). Tilt and azimuth angles in solar energy applications – A review. *Renewable and Sustainable Energy Reviews*, 77(September), 147–168. <https://doi.org/10.1016/j.rser.2017.03.131>
- Hill, C. (1976). *March 1976. March*, 151–154.
- Intelligetn Energy Europe. (2012). *A GUIDE TO THE STANDARD EN12975 Quality assurance in solar heating and cooling technology*.
- Khan, B. (2012). *Wireless sensor networking using AADI Sensors with WSN Coverage*.
- Kocer, A., Yaka, I., Sardogan, G., & Gungor, A. (2015). Effects of Tilt Angle on Flat-Plate Solar Thermal Collector Systems. *British Journal of Applied Science & Technology*, 9(1), 77–85. <https://doi.org/10.9734/bjast/2015/17576>

- Koprivica, B., Milovanovic, A., & Dlabac, T. (2018). An approach to cold junction compensation and identification of unknown thermocouple type. *Revue Roumaine Des Sciences Techniques Serie Electrotechnique et Energetique*, 63(3), 277–282.
- Laurila, H. (2017). *Thermocouple Cold Junction Compensation*. September. <https://blog.beamex.com/thermocouple-cold-junction-compensation>
- Manual, T. N. U. (2003). *Traditional NI-DAQ User Manual*. 370696.
- More, S. A. (2014). *Analog Approach*. August, 1–7.
- National Instrument Team. (2015). *User Guide Ni Usb-6008/6009*. 1–26. <http://www.ni.com/pdf/manuals/371303n.pdf>
- Peeters, F., Peetermans, M., & Indesteege, L. (2010). Temperature Sensors. *Modern Sensors Handbook*, 347–393. <https://doi.org/10.1002/9780470612231.ch8>
- Psikuta, A., Niedermann, R., & Rossi, R. M. (2014). Effect of ambient temperature and attachment method on surface temperature measurements. *International Journal of Biometeorology*, 58(5), 877–885. <https://doi.org/10.1007/s00484-013-0669-4>
- Rojas, D., Beermann, J., Klein, S. A., & Reindl, D. T. (2008). Thermal performance testing of flat-plate collectors. *Solar Energy*, 82(8), 746–757. <https://doi.org/10.1016/j.solener.2008.02.001>
- Sheet, D., Sealed, E., Mass, T., & Meters, F. (2014). *SLA5800 Series*. 1–12.
- Started, G., & Material, S. (2005). Getting Started with Getting Started with. *Group, May*, 1–72.
- Susmitha, P., & Sowya Bala, G. (2014). Design and Implementation of Weather Monitoring and Controlling System. *International Journal of Computer Applications*, 97(3), 19–22. <https://doi.org/10.5120/16987-7089>
- Thepnurat, M., Saphet, P., & Tong-On, A. (2018). Low-Cost DIY Vane Anemometer based on LabVIEW interface for Arduino. *Journal of Physics: Conference Series*, 1144(1). <https://doi.org/10.1088/1742-6596/1144/1/012028>
- Thornsberry, C. (1989). Methicillin-resistant staphylococci. In *Clinics in Laboratory Medicine* (Vol. 9, Issue 2). [https://doi.org/10.1016/s0272-2712\(18\)30627-9](https://doi.org/10.1016/s0272-2712(18)30627-9)
- Zaaiman, W. (2012). *Solar Irradiance and Photovoltaic Measurements From Solar Radiation to PV Arrays*.